Accepted Manuscript

Glucose addition increases the magnitude and decreases the age of soil respired carbon in a long-term permafrost incubation study

Elaine Pegoraro, Marguerite Mauritz, Rosvel Bracho, Chris Ebert, Paul Dijkstra, Bruce A. Hungate, Kostas T. Konstantinidis, Yiqi Luo, Christina Schädel, James M. Tiedje, Jizhong Zhou, Edward A.G. Schuur

Please cite this article as: Pegoraro, E., Mauritz, M., Bracho, R., Ebert, C., Dijkstra, P., Hungate, B.A., Konstantinidis, K.T., Luo, Y., Schädel, C., Tiedje, J.M., Zhou, J., Schuur, E.A.G., Glucose addition increases the magnitude and decreases the age of soil respired carbon in a long-term permafrost incubation study, *Soil Biology and Biochemistry* (2018), doi: https://doi.org/10.1016/j.soilbio.2018.10.009.
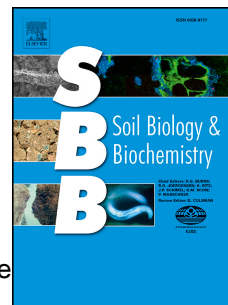
1 Title: Glucose addition increases the magnitude and decreases the age of soil respired
2 carbon in a long-term permafrost incubation study
3
4 Authors: Elaine Pegoraro[a,b], Marguerite Mauritz[a,b], Rosvel Bracho[c], Chris Ebert[a,b], Paul
5 Dijkstra[a,b], Bruce A. Hungate[a,b], Kostas T. Konstantinidis[d], Yiqi Luo[a,b,e,g], Christina
6 Schädel[a,b], James M. Tiedje[f], Jizhong Zhou[g], and Edward A.G. Schuur[a,b].
7
8 Affiliations:
9 [a]Department of Biological Sciences, Northern Arizona University, Flagstaff, AZ 86011,
10 USA
11 [b]Center for Ecosystem Science and Society, Northern Arizona University, Flagstaff, AZ
12 86011, USA
13 [c]School of Forest Resources & Conservation, University of Florida, Gainesville, FL 32611,
14 USA
15 [d]School of Civil and Environmental Engineering and School of Biology, Georgia Institute
16 of Technology, Atlanta, Georgia 30332, USA
17 [e]Department of Earth System Science, Tsinghua University, Beijing 100084, China
18 [f]Department of Plant, Soil and Microbial Sciences, Center for Microbial Ecology,
19 Michigan State University, East Lansing, Michigan 48824, USA
20 [g]Department of Microbiology and Plant Biology, University of Oklahoma, Norman,
21 Oklahoma 73019, USA
22
23
24 Corresponding author: Elaine Pegoraro, (407) 412 8881, efp23@nau.edu
25

27 **Abstract**

28 Higher temperatures in northern latitudes will increase permafrost thaw and stimulate
29 above-and belowground plant biomass growth in tundra ecosystems. Higher plant
30 productivity increases the input of easily decomposable carbon (C) to soil, which can
31 stimulate microbial activity and increase soil organic matter decomposition rates. This
32 phenomenon, known as the priming effect, is particularly interesting in permafrost
33 because an increase in C supply to deep, previously frozen soil may accelerate
34 decomposition of C stored for hundreds to thousands of years. The sensitivity of old
35 permafrost C to priming is not well known; most incubation studies last less than one
36 year, and so focus on fast-cycling C pools. Furthermore, the age of respired soil C is
37 rarely measured, even though old C may be vulnerable to labile C inputs. We incubated
38 soil from a moist acidic tundra site in Eight Mile Lake, Alaska for 409 days at 15°C. Soil
39 from surface (0-25 cm), transition (45-55 cm), and permafrost (65-85 cm) layers were
40 amended with three pulses of uniformly ^{13}C labeled glucose or cellulose, every 152 days.
41 Glucose addition resulted in positive priming in the permafrost layer 7 days after each
42 substrate addition, eliciting a two-fold increase in cumulative soil C loss relative to
43 unamended soils with consistent effects across all three pulses. In the transition and
44 permafrost layers, glucose addition significantly decreased the age of soil-respired CO_2-C
45 with Δ^{14}C values that were 115‰ higher. Previous field studies that measured the age
46 of respired C in permafrost regions have attributed younger Δ^{14}C ecosystem respiration
47 values to higher plant contributions. However, the results from this study suggest that
48 positive priming, due to an increase in fresh C supply to deeply thawed soil layers, can
49 also explain the respiration of younger C observed at the ecosystem scale. We must
50 consider priming effects to fully understand permafrost C dynamics, or we risk
51 underestimating the contribution of soil C to ecosystem respiration.

1. Introduction

Temperatures in northern latitudes are currently increasing by 0.6°C each decade, a rate that is two times higher than the global average (IPCC, 2013). Higher temperatures can thaw permafrost (Brown and Romanovsky, 2008; Romanovsky et al., 2010; Harden et al., 2012; Romanovsky et al., 2012) and expose previously protected soil organic matter (SOM) to microbial decomposition (Schuur et al., 2015). Though the permafrost region encompasses only 15% of the total global soil area, it stores two times more carbon (C) than the atmosphere: 1,330–1,580 petagrams C (Pg; 1 Pg = 1 billion metric tons) (Zimov et al., 2006; Tarnocai et al., 2009; Hugelius et al., 2014; Schuur et al., 2015). Microbial mineralization of this stored C can exacerbate the effects of climate change by increasing greenhouse gas concentrations in the atmosphere in the form of carbon dioxide (CO_2) and methane (Schuur et al., 2008).

The mineralization rate of permafrost C is partially controlled by its inherent decomposability (Schädel et al., 2014; Schuur et al., 2015). Upon thaw, permafrost C is mobilized (Schuur et al., 2009; Nowinski et al., 2010), and overall soil C losses are high because of the high biolability of organic C in initial stages of decomposition (Dutta et al., 2006; Vonk et al., 2013). However, that initial C is quickly mineralized, and microbes are left with a much larger pool of slowly decomposing C. A previous soil incubation study found that > 85% of the fast decomposing C is depleted after ~ 3 months of incubation at 15°C (Bracho et al., 2016), but it amounts to less than 5% of all C in both organic and mineral soil layers (Schädel et al., 2014). Although soil C comprises several different pools with turnover times spanning less than a year to several hundred years

3

74 (Trumbore, 2000), the majority of the C stored in permafrost is old (Zimov et al., 2006;

75 Schuur et al., 2009). Therefore, we expect that long-term C losses will largely originate

76 from old and slowly decomposing C pools (Schuur et al., 2008; Knoblauch et al., 2013;

77 Schädel et al., 2013; Schädel et al., 2014).

78   Slowly decomposing C that accumulated over hundreds to thousands of years in

79 permafrost (Czimczik and Welker, 2010; Pries et al., 2012) is thought to be relatively

80 energy-poor. A long-term (~ 1 year) permafrost incubation study revealed that less than

81 3% of the initial soil bulk C is mineralized in the absence of substrate inputs (Dutta et al.,

82 2006). Without an energy source in the form of fresh organic C, microbial activity

83 decreases (Schimel and Weintraub, 2003); however, this energy limitation can

84 potentially be lifted with an increased input of labile C to soil (De Nobili et al., 2001;

85 Fontaine et al., 2007; Blagodatskaya and Kuzyakov, 2008).

86   A warmer climate will also increase shrub expansion in tundra ecosystems, which

87 will increase plant productivity and litter input to soil (Chapin et al., 1995; Shaver et al.,

88 2000; Tape et al., 2006; Natali et al., 2012). Priming theory suggests that a greater

89 supply of fast decomposing C from leaf and root litter, root exudates, and dissolved

90 organic C leachate can increase microbial decomposition of native SOM (Bingeman et

91 al., 1953). Studies show that microbes utilize fresh C as an energy source to produce

92 enzymes that assist in the decomposition of organic molecules that are resistant to

93 microbial degradation (Schimel and Weintraub, 2003; Fontaine et al., 2007; Bernal et al.,

94 2016). Some studies have investigated the implication of tundra shrub expansion on

95 SOM decomposition by adding glucose or low molecular weight C to soil, and found no

96   effects of priming (Rousk et al., 2016; Lynch et al., 2018). However, these studies

97   amended surface and O-horizon soils exclusively, which do not reflect the potential

98   priming effects of deep-rooting tundra species (e.g. *R. chamaemorus and E. vaginatum*)

99   whose roots extend to the thaw-front (>45 cm) (Keuper et al., 2017), and thus may

100   increase C input to deep soils and recently thawed permafrost.

101   Priming is a particularly interesting phenomenon in permafrost soil because frozen

102   ground is impermeable to dissolved organic C (DOC) infiltration (Walvoord and Kurylyk,

103   2016). Environmental changes that increase C inputs in deep soil can increase soil C

104   vulnerability to decomposition and loss (Bernal et al., 2016). This means that as

105   permafrost thaws, soil in deep layers may receive fresh C inputs during rain and snow

106   events for the first time in hundreds to thousands of years. Previous studies modeling

107   water movement through soil with underlying permafrost show that DOC input to

108   deeper layers releases more CO_2 (Fan et al., 2013). Fresh C input to soil will also be

109   accompanied by pulses of mineralized N upon permafrost thaw (Rustad et al., 2001;

110   Keuper et al., 2012; Salmon et al., 2018), which could create an ideal environment for

111   higher microbial activity.

112   A more active microbial community, especially in deep soil layers, can alter soil C

113   dynamics by increasing decomposition of old and slowly decomposing organic C, and

114   accelerate C turnover rates (Fontaine et al., 2007; Paterson et al., 2009). While the

115   stability of old soil C can change in the presence of labile C inputs (Fontaine et al., 2007;

116   Bernal et al., 2016), permafrost priming studies have not measured the age of soil

117   respired C. Furthermore, most incubation studies are conducted in short-term

118 laboratory incubations (< 1 year), and thus only focus on fast-cycling soil C pools (Fan et

119 al., 2013; Wild et al., 2014; Wild et al., 2016). To fully understand permafrost C dynamics

120 and priming effects, we measured the magnitude of soil C loss and the age of respired C.

121   We hypothesized that amending permafrost soil with multiple pulses of glucose,

122 the most abundant sugar in rhizodeposits (Derrien et al., 2004), or cellulose, the most

123 common polymer in plant litter (Kögel-Knabner, 2002), would: (1) increase soil C

124 decomposition (positive priming), particularly in permafrost where the majority of the C

125 is slow decomposing C (Schädel et al., 2014), (2) sustain higher rates of soil C

126 decomposition over the long-term because microbes will readily use substrates as an

127 energy source following each pulse, and (3) increase the proportion of old C that is

128 respired as a result of soil priming because it comprises the bulk of the soil C pool in

129 permafrost (Schuur et al., 2009).

130 **2.   Materials and Methods**

131 *2.1.   Site Description*

132   Soil cores were sampled in 2013 from Eight Mile Lake, Alaska (63° 52' 59"N, 149°

133 13' 32"W), where the mean annual temperature is -1.0 $^{\circ}$C, and the mean annual

134 precipitation is 378 mm (Schuur et al., 2009). The site is situated on a well-drained,

135 northeast-facing hillslope (700 m) (Natali et al., 2011) in the discontinuous permafrost

136 zone, but is underlain entirely by permafrost (Osterkamp et al., 2009). Though our site is

137 in the subarctic, it exemplifies a region vulnerable to permafrost degradation that is

138 analog to projected conditions in the Arctic as temperatures increase. The site has

139 cryoturbated mineral soil, comprising glacial till and windblown loess, with dominant

6

140   amounts of quartz and feldspars. The soil type is Gelisol (Soil Survey Staff, 2014) with an

141   organic horizon ~35 cm thick, and C concentrations greater than 20% (Natali et al., 2011;

142   Pries et al., 2012; Plaza et al., 2017b). In 2013, the maximum thaw depth at the peak of

143   the growing season was < 65 cm (Mauritz et al., 2017). The vegetation is moist acidic

144   tundra, dominated by *Eriophorum vaginatum*. Plant species composition includes

145   *Vaccinium uliginosum, Carex bigelowii, Betula nana, Rubus chamaemorus, Empetrum*

146   *nigrum, Rhododendron subarcticum, V. vitis-idaea, Andromeda polifolia* and *Oxycoccus*

147   *microcarpus*. Nonvascular plant cover contains feather moss (primarily *Pleurozium*

148   *schreberi)* and *Sphagnum* species, as well as several lichen species (primarily *Cladonia*

149   spp.) (Schuur et al., 2007; Natali et al., 2011; Deane-Coe et al., 2015).

150   *2.2.   Soil Core Collection and Processing*

151   Four soil cores were collected in June 2013. The seasonally thawed surface soil was

152   cut using a serrated knife, and the underlying frozen soil was cored using a Tanaka drill

153   with a 7.6 cm diameter hollow bit. Soil was sampled to the depth at which the corer hit

154   rocks (~ 85 cm). Cores were wrapped in aluminum foil, kept frozen for shipment, and

155   stored until the start of the experiment.

156   In the lab, the surface vegetation was clipped off, and cores were sectioned to 15

157   cm at the surface and 10 cm increments thereafter (0-15 cm, 15-25 cm, etc.) to the end

158   of the core. The organic/mineral horizon demarcation was determined by %C analysis

159   (mineral < 20% C). Rocks were removed, and we accounted for their mass and volume in

160   bulk soil density calculation. Each depth increment was subsampled for moisture

161   content, and bulk %C, %N, and $\delta^{13}C$ (‰). Bulk C and N concentrations were determined

162   by dry combustion using a Costech Analytical ECS 4010 elemental analyzer (Valencia, CA,

163   USA) (Pries et al., 2012). Stable C isotope data were determined using a Thermo

164   Finnigan Delta V Advantage continuous flow isotope ratio mass spectrometer

165   (ThermoScientific Inc., Waltham, MA, USA). Soil pH was determined using the slurry

166   method with a 1:1 ratio by proportional weight of soil to deionized water. Soil pH was

167   measured using an Orion 2 Star pH Benchtop (ThermoScientific Inc., Waltham, MA,

168   USA).

169   We measured initial microbial biomass on a subsection of soil that was not

170   incubated. Due to constrains in soil availability, only 3 cores at depths 0-15, 15-25 and

171   45-55 cm, and only 2 cores at 75-85 cm were extracted; we did not have enough soil

172   available for extraction at 65-75 cm. Four analytical replicate samples (4-6 g soil) from

173   each individual core and depth increment were homogenized, and soils were extracted

174   with 25 ml 2M KCl. Two of the replicates were amended with 0.25 ml chloroform to lyse

175   microbial cell membranes. Samples were shaken for 1 hour, then vacuum filtered

176   through pre-leached Whatman GF/A filters. Extracts were sparged with air for 30

177   minutes to volatilize chloroform, and frozen for storage. Dissolved organic C

178   concentrations were measured using a Shimadzu TOC-L analyzer (Kyoto, Japan), and

179   microbial biomass C was calculated as the difference in DOC between extracts

180   performed with and without chloroform (Salmon et al., 2018).

181   *2.3.   Incubation*

182   We incubated soil from five different depths, representative of the surface layer (0-

183   15 and 15-25 cm), the organic/mineral transition layer (45-55 cm), and the permafrost

184   layer (65-75 and 75-85 cm), from 4 replicate soil cores. We weighed triplicates (~ 80 g

185   wet weight) from each depth into 1 L Mason jars and assigned each jar to a treatment:

186   unamended (control), glucose, or cellulose (4 cores x 5 depth x 3 treatments = 60 jars).

187   We pre-incubated all samples for 4 weeks at 15°C so that waterlogged soils from

188   ice-rich sections (65-75 and 75-85 cm) could air dry to less than 60% water holding

189   capacity (WHC). At the end of the 4 weeks, we amended our samples with uniformly ^{13}C

190   labeled glucose U-13C6, 24-25 atom% (Cambridge Isotope Laboratories Inc., Andover,

191   MA, USA) or cellulose 97 atom% D from maize (Sigma-Aldrich Co., St. Louis, MO, USA).

192   Soils were amended with 3.5 mg substrate C per gram of initial soil C to account for

193   differences in initial bulk soil %C in each layer. The total concentration added

194   corresponded to 23-84% of the annual net primary productivity (NPP) in our site, scaled

195   to a per gram soil basis (Natali et al., 2012). Labeled substrates were mixed with

196   unlabeled glucose or cellulose (Sigma Life Science, St. Louis, MO, USA) for more diluted

197   δ^{13}C values (Supplemental Table 1). Deionized water was added to the mixtures of finely

198   ground glucose or cellulose so that substrate solutions could be injected in each soil

199   section with a syringe to minimize soil disturbance and maximize distribution.

200   Unamended soils received deionized water only. Moisture was adjusted to ~ 60% WHC

201   throughout the incubation in all treatments. Soils were aerobically incubated and

202   maintained at 15°C. A second and third amendment pulse was added at day of

203   incubation (DOI) 153 and 305 (every 152 days). We chose to amend soils every 152 days

204   because Bracho et al. (2016) found that 85-95% of fast-decomposing C is depleted

205 within 100 days of incubation at 15°C; therefore, we assumed most of the added

206 substrate would be consumed before the next C addition.

207 *2.4.   Flux and isotope measurements*

208   Carbon dioxide and $\delta^{13}C$ measurements were coupled and measured daily for the

209 first week following each pulse, every 2 days for the second week, and once every ~4

210 weeks until the next amendment.

211   Jars were placed in a water bath set to 15°C, connected to an automated soil

212 incubation system (ASIS) that sequentially measured CO_2 concentration in each jar by

213 circulating air through an infrared gas analyzer (IRGA) at 0.9 L min^{-1} (Li-820 Licor,

214 Lincoln, Nebraska). Pressure and CO_2 concentrations in each jar were recorded on a data

215 logger (CR1000, Campbell Scientific, Logan UT) every three seconds for 8 minutes.

216 Carbon dioxide flux, in micrograms of C per gram of initial soil C per day, was calculated

217 as the rate of CO_2-C increase in the headspace of each jar over 3-4 cycles that lasted 8.5

218 hours each. ASIS is a closed-loop system, but individual jar fluxes were corrected for

219 carry over CO_2 based on the CO_2 concentration in the previous jar and the carry over

220 volume, which included the tubbing, IRGA, flow mass controlled, and pump. Details of

221 ASIS are described in Bracho et al. (2016).

222   After each flux measurement, jar headspace was scrubbed for 5 minutes with soda

223 lime and incubated at 15°C for a couple of hours to allow CO_2 to accumulate. We

224 measured $\delta^{13}CO_2$-C on a Picarro G2201-*i* Isotopic CO_2/CH_4 cavity ring-down

225 spectrometer (Picarro Inc., Sunnyvale, California, USA) and recorded the 2-minute

226 $\delta^{13}CO_2$-C average for each jar at the end of a 4-minute measurement period. We

227   allowed the Picarro cavity to return to ambient $^{13}CO_2$ levels before measuring each jar,

228   and we frequently used a reference CO_2 gas before and after measurements for

229   calibration (Airgas, ASG Los Angeles, CA).

230   Because of the high number of jars, the incubation was conducted in 2 rounds,

231   staggered in time to manage the high volume of measurements. Each round was treated

232   the same, and treatments were fully interspersed between rounds.

233   *2.5.   Priming calculations*

234   In the amended treatments, total CO_2-C flux was a combination of soil-derived C

235   and substrate-derived C, so we applied an isotopic mass balance equation to partition

236   soil-derived C (SOC) from substrate-derived C:

237        $C_{SOC} = C_{total} (\delta_{total} - \delta_{substrate}) / (\delta_{SOC} - \delta_{substrate})$ (1)

238   where C_{SOC} is the soil-respired C, C_{total} is total C respired in substrate-amended soils,

239   which includes soil-derived C and substrate-derived C, δ_{total} is the total $\delta^{13}CO_2$-C

240   respired, which includes soil-derived $\delta^{13}C$ and substrate-derived $\delta^{13}C$, $\delta_{substrate}$ is the δ

241    $^{13}CO_2$-C from the added substrate (end-member), and δ_{SOC} is the soil-respired $\delta^{13}CO_2$-C

242   from unamended samples (end-member). Priming was calculated as the difference in

243   soil-respired C in amended samples and soil-respired C in unamended samples (Mau et

244   al., 2015). A positive value indicated that more soil C was mineralized in amended soils

245   relative to control (i.e. positive priming). A negative value indicated that less soil C was

246   mineralized in amended soils relative to control (i.e. negative priming). All values were

247   reported as micrograms of respired C per gram of initial soil C.

11

248   Though we amended soils with cellulose in Pulse 1, the dilution of the labeled

249   substrate with unlabeled cellulose made the $\delta^{13}C$ signature too similar to that of the

250   soil; therefore, we were unable to use the substrate end-member to calculate priming.

251   For pulses 2 and 3, we used a cellulose substrate with a higher $\delta^{13}C$ signature

252   (Supplemental Table 1). We only analyzed and interpreted cellulose data for pulses 2

253   and 3.

254   To calculate substrate use, or the amount of substrate that was respired after each

255   pulse, we implemented a mass balance equation to partition substrate-derived C

256   ($C_{substrate}$) from the total C respired (C_{total}):

257    $$C_{substrate} = C_{total} (\delta_{total} - \delta_{soil}) / (\delta_{substrate} - \delta_{soil}) \tag{2}$$

258   We calculated the cumulative $C_{substrate}$ respired after each pulse as a percent of the

259   added substrate (3.5 mg $C_{substrate}$ g^{-1} C) by linearly interpolating the respired $C_{substrate}$

260   values and integrating the entire sampling period of 105 days.

261   *2.6.   Radiocarbon*

262   To determine the age of respired soil C, we sampled $\Delta^{14}CO_2$ at DOI 15 and 105 after

263   pulse 1, and DOI 319 (i.e. day 15 after pulse 3). The headspace in each jar was scrubbed

264   free of CO_2 using soda lime to remove any background atmospheric CO_2 contributions.

265   After allowing each headspace to accumulate between 0.5-1.0 mg C, based on the most

266   recent flux rates measured, we collected CO_2 in zeolite molecular sieve traps (Alltech

267   13X; Alltech Associates, Deerfield, IL, USA) for 5 minutes (Hardie et al., 2005). Each

268   molecular sieve trap was baked at 650 °C to desorb CO_2 (Bauer et al., 1992). Carbon

269   dioxide was cryogenically purified using liquid nitrogen, and reduced to graphite by H_2

270   reduction with an Fe catalyst on a vacuum line (Vogel et al., 1987). Graphite samples

271   were sent to the UC Irvine W.M. Keck carbon cycle accelerator mass spectrometry

272   (AMS) laboratory for $\Delta^{14}C$ analysis. Radiocarbon samples are analyzed with the standard

273   oxalic acid II, and the precision of an AMS measurement is $\pm$ 2‰, but for many

274   applications this error is smaller than sampling error (Trumbore et al., 2016b).

275   Radiocarbon values in unamended samples were corrected for mass-dependent

276   fractionation to a $\delta^{13}C$ value of -25 ‰, which is routinely done to natural abundance

277   samples (Stuiver and Polach, 1977; Trumbore et al., 2016a). For samples amended with

278   enriched ^{13}C substrates, the increase in ^{13}C atoms relative to ^{12}C is not due to mass-

279   dependent isotopic fractionation—that is, ^{14}C is not enriched, only ^{13}C is. Therefore,

280   using $\delta^{13}C$ = -25‰ as a fractionation correction would yield an inaccurate $\Delta^{14}C$. Thus,

281   we applied the correction described in Torn and Southon (2001), using the measured

282    $\delta^{13}C_{substrate}$ value as a proxy for the isotopic fractionation correction.

283   Amended samples had a $\Delta^{14}C$ signature from combined soil and substrate respired

284   C; therefore, we calculated the soil respired $\Delta^{14}C$ fraction (*f*) using $\delta^{13}C$ signatures of the

285   substrate and SOC with a similar mass-balance equation implemented in the priming

286   calculation:

287         $f = (\delta_{total} - \delta_{substrate}) / (\delta_{SOC} - \delta_{substrate})$ (3)

288   where δ_{total} is the total $\delta^{13}CO_2$-C respired, $\delta_{substrate}$ is the $\delta^{13}CO_2$-C from the added

289   substrate (end-member), and δ_{SOC} is the soil-respired $\delta^{13}CO_2$-C from control samples

290   (end-member). We then applied the *f* of soil respired $\Delta^{14}C$ to the following equation:

291         $\Delta^{14}C_{SOC} = \Delta^{14}C_{total} - ((1-f) * \Delta^{14}C_{substrate})/f$ (4)

292   This soil respired $\Delta^{14}C$ fraction (*f*) allows us to calculate the true $\Delta^{14}C$ value of soil

293   respiration ($\Delta^{14}C_{SOC}$) by removing any substrate contribution ($\Delta^{14}C_{substrate}$) from the $\Delta^{14}C$

294   measured by the AMS ($\Delta^{14}C_{total}$) (Schuur and Trumbore, 2006). The $\Delta^{14}C_{substrate}$ was

295   10.1‰ and 62.3‰ for glucose and cellulose, respectively.

296   *2.7.   Statistical Analysis*

297   Statistical analyses of the main effects and interactions on response variables were

298   performed in R (R Development Core Team, 2015) using linear mixed effects models,

299   lme4 package (Bates et al., 2015). To meet normality assumptions, data were log-

300   transformed when necessary. We removed 6 outlier priming ($\mu g\ CO_2$-C $g^{-1}C$) values out

301   of 1347 values (<1% of the data). Normality and homoscedasticity were visually

302   examined using residual plots.

303   Samples from each core (n=4) were measured at 5 different depths (0-15, 15-25,

304   45-55, 65-75, and 75-85 cm), but the data were analyzed by pooling depth increments

305   into 3 layers: surface (0-15 and 15-25 cm), transition (45-55 cm), and permafrost (65-75

306   and 75-85 cm) based on statistically similar initial bulk soil %C. Analyzes were performed

307   by including soil layer nested in soil core as a random effect so that depth increments

308   would not be treated as independent replicates. Initial soil properties were tested by

309   incorporating soil layer as a fixed effect, and a random effect of soil layer nested in soil

310   core. A post-hoc Tukey HSD test was used to determine significant differences between

311   layers.

312   Priming ($\mu g\ CO_2$-C $g^{-1}C$) was tested in response to soil layer, pulse, day(s) after pulse

313   (DAP), and their interactions. Analyses included a random effect of jar nested in soil

14

314   layer, nested in core, to account for repeated measurements. We accounted for round

315   (n = 2) as a random effect in our model, but it had no effect on variance, so we dropped

316   the random effect term. We fit separate models for glucose priming and cellulose

317   priming to avoid an unbalanced design because cellulose data was missing in pulse 1.

318   Changes in cumulative soil C loss in the first week after each pulse were calculated as

319   the response ratio—the ratio between samples amended with glucose and

320   corresponding unamended samples.

321   Soil respired $\Delta^{14}C$ (‰) was tested in response to treatment, layer, and DOI.

322   Analyses also included a random effect of jar nested in layer, nested in core. We did not

323   have to analyze glucose and cellulose independently because we had radiocarbon data

324   for both treatments for the three different sampling periods. However, to meet

325   conditions of homoscedasticity, we analyzed surface layer samples independently from

326   transition and permafrost layers. Surface soils have C stocks that are more homogenous,

327   and have positive $\Delta^{14}C$ (‰) values that correspond to modern C that contain elevated

328   'bomb' $\Delta^{14}C$ values (Turnbull et al., 2016), whereas transition and permafrost layers are

329   more heterogeneous due to cryoturbation, soil subsidence, and soil formation (Harden

330   et al., 2012), and have negative $\Delta^{14}C$ (‰) values as a result of radioactive decay

331   (Turnbull et al., 2016).

332   We used a Backward step-wise model selection to eliminate fixed effects that

333   increased AIC values by 5 or more. Ninety-five percent confidence intervals (CI) for fixed

334   effects were obtained by bootstrapping parameter estimates (1000 iterations). A fixed

335   effect was considered significant if the 95% CI did not include zero (Pinheiro and Bates,

336   2000).

337   **3.   Results**

338   *3.1.   Soil properties*

339   Soil properties significantly differed between soil layers (Table 1). Initial bulk soil C

340   and N concentrations significantly decreased with depth; concentrations in the surface

341   were almost 2 times higher than the transition layer, and 4 times higher than the

342   permafrost layer, but there were no significant differences in C:N. Bulk density was

343   significantly lower in the surface, but was not different between the transition and

344   permafrost layers. Carbon concentrations decreased from about 38% in the surface to

345   21% in the transition, and to less than 10% in the permafrost layer. Initial bulk $\delta^{13}C$

346   values were significantly higher in the surface layer, but did not differ between the

347   transition and permafrost layers. Initial microbial biomass was not significantly different

348   between layers, but was marginally higher in the surface (1.22 mg C g^{-1} soil C) than the

349   transition (0.36 mg C g^{-1} soil C) and permafrost layers (0.66 mg C g^{-1} soil C). Soil pH was

350   in the acidic range, and significantly increased with depth.

351   *3.2.   Priming effects*

352   The addition of glucose elicited immediate priming responses in both surface and

353   permafrost layers, though these responses differed in sign and magnitude. Priming in

354   the surface layer was mostly negative in the first week after each pulse. We observed

355   significantly negative priming 48h after each glucose amendment (Surface x 2 DAP: CI -

16

356   77.36 µg CO_2-C g^{-1}C to -9.09 µg CO_2-C g^{-1}C, Fig. 1, Supplemental Table 2) with consistent

357   effects in all pulses.

358   In the permafrost layer, glucose addition resulted in significant positive priming

359   effects that lasted 7 days after each pulse; this response was similar across all three

360   pulses (Fig. 1, Supplemental Table 2). This strong priming effect in the glucose treatment

361   doubled the cumulative soil C loss relative to the unamended permafrost layer; the

362   cumulative response ratio of soil C loss in glucose treatments relative to control was

363   close to 2 (Figure 2). There were no significant priming responses in the transition layer,

364   with consistent effects across all three pulses and DAP, although mean values generally

365   showed positive or no priming effects (Fig. 1, Supplemental Table 2).

366   Cellulose amendments resulted in positive and negative priming responses

367   depending on the soil layer, and in general had a longer, albeit smaller effect on soil C

368   loss than did glucose. In the surface soil, the 3rd cellulose pulse induced significant

369   negative priming that lasted the entire sampling period (Surface x Pulse 3: CI -49.41 to -

370   34.94 µg CO_2-C g^{-1}C, Fig. 3, Supplemental Table 2). In the permafrost layer, the 3rd

371   cellulose pulse led to significant positive priming that increased soil C loss (Permafrost x

372   Pulse 3: CI 7.66 to 28.67 µg CO_2-C g^{-1}C, Fig. 3, Supplemental Table 2). As with glucose

373   addition, there were no significant priming effects in the transition layer, but mean

374   responses trended towards positive or no priming effects (Fig. 3, Supplemental Table 2).

375   *3.3.   Age of respired soil C*

376   In unamended soils, the Δ^{14}C value of respired C became more negative with depth,

377   indicating that microbes respired older soil C deeper in the soil profile (Fig. 4). Over the

17

378 course of the incubation, soil respired Δ^{14}C averaged 42‰ in the surface layer

379 (Intercept: CI 35‰ to 50‰, Table 2), -201‰ in the transition layer (Intercept: CI -296‰

380 to -110‰, Table 2), and -426‰ in the permafrost layer (Permafrost x DOI 15: CI -516‰

381 to -334‰, Table 2) (Figure 4). We observed the highest variability in soil-respired Δ^{14}C in

382 the permafrost horizon; the respired Δ^{14}C soil signature in the unamended permafrost

383 layer was significantly more positive on DOI 105 relative to DOI 15, (Permafrost x DOI

384 105: CI -420‰ to -231‰, Table 2), but by the end of the incubation, the soil-respired

385 Δ^{14}C was once again similar to DOI 15 (Permafrost x DOI 319: CI -497‰ to -307‰, Table

386 2).

387   Glucose treatments significantly increased the Δ^{14}C value of soil respired C by

388 115‰ (Glucose: CI 25‰ to 206‰, Table 2) in the transition and permafrost layers

389 relative to unamended soils in the transition layer (Fig. 4). This means that glucose

390 addition induced soil C mineralization of relatively young C in deeper layers. In the

391 surface layer we saw a similar pattern, soil respired Δ^{14}C values in the glucose treatment

392 were closer to 0‰, which indicates soil respired C was younger relative to unamended

393 soils; however, this difference was not statistically significant. Cellulose did not change

394 the Δ^{14}C of respired CO_2 relative to unamended soils.

395 *3.4.   Substrate use*

396   Not all the substrate C added was respired by the end of each pulse. The amount

397 of glucose C respired, as a percent of added substrate 105 DAP, was 40-54% in the

398 surface, 37-58% in the transition, and 68-126% in the permafrost layer (Table 3). Out of

399 the total glucose C respired in the permafrost layer 105 DAP, 20-47% was mineralized in

18

400 the first week, when we observed significant positive priming effects (Table 4), we also

401 observed the highest CO_2 fluxes and $\delta^{13}CO_2$ in the first 7 DAP that often decreased to

402 match unamended concentrations 15 DAP (Supplemental Figures 1 and 2). The

403 cumulative amount of cellulose loss for pulses 2 and 3 ranged from 20-26% in the

404 surface, 16-25% in the transition, and 9-12% in the permafrost layer (Table 3). The

405 cellulose treatment did not elicit a high peak in CO_2 fluxes in the first 7 DAP

406 (Supplemental Figure 3), and $\delta^{13}CO_2$ did not decrease to match unamended values 105

407 days after pulses 2 and 3 (Supplemental Figure 4).

408 **4.   Discussion**

409   Models forecast that 5-15% of the terrestrial permafrost C pool (~130-160 Pg C) is

410 vulnerable to decomposition in this century under current warming trajectories (Schuur

411 et al., 2015). Higher temperatures will also increase shrub expansion in tundra regions

412 (Chapin et al., 1995; Tape et al., 2006), and total belowground plant biomass, root

413 production, and rooting depth (Sullivan et al., 2007; Zamin et al., 2014; Keuper et al.,

414 2017), thus increasing fresh C inputs to soil. Our findings show that adding glucose to

415 permafrost soils can change the magnitude and age of respired soil C.

416 *4.1.   Permafrost soil C loss increases with glucose addition*

417   Glucose additions caused a two-fold increase in permafrost soil C loss relative to

418 unamended samples in the first week after each pulse. The additional soil C mineralized

419 in the permafrost layer 7 days after each pulse was 0.71 to 1.20 mg C g^{-1}C, which is 1 to

420 almost 2 times greater than the initial microbial biomass in that layer (0.66 mg C g^{-1} C).

421 This suggests that the increase in C loss resulted primarily from an increase in SOM

19

422   decomposition (real priming effect), rather than an accelerated turnover of the

423   microbial C pool (apparent priming effect) (Blagodatskaya and Kuzyakov, 2008;

424   Blagodatskaya et al., 2011). A previous priming incubation study in Siberian permafrost

425   conducted over 6 days also reported a two-fold increase in SOM decomposition in deep

426   mineral soils amended with glucose (Wild et al., 2014). De Baets et al. (2016) similarly

427   reported significant positive priming effects on a 10-day glucose addition study

428   conducted in tussock tundra mineral soil and permafrost. Our results corroborate the

429   hypothesis that the addition of an easily decomposable C substrate alleviates energy

430   constraints in deeper soil layers that have higher concentrations of slowly decomposing

431   C.

432   We hypothesized that amending deeper soil layers with a simple substrate would

433   increase soil C decomposition because slowly decomposing C constitutes most of the C

434   at depth. Our initial soil parameters show that the fraction of slowly-decomposing C

435   increased in the permafrost layer. We observed lower bulk soil δ^{13}C values at depth,

436   which are common for soils that are waterlogged, and can indicate the accumulation of

437   recalcitrant materials, like lignin (Alewell et al., 2011). The increased fraction of slowly-

438   decomposing C in deeper layers was also reflected in the nuclear magnetic resonance

439   spectra (NMR) analyses performed on subsamples of our soil cores. We found that the

440   proportion of alkyl C relative to *O*-alkyl C increased in the permafrost layer (Plaza et al.,

441   2017a). This pattern in the alkyl/*O*-alkyl ratio represents progressive organic matter

442   degradation, and decreased plant-derived fresh organic matter relative to microbial

443   biomolecules (Baldock and Skjemstad, 2000).

444   The negative priming effects in the surface layer that we observed after each

445   glucose pulse can be attributed to a switch from microbial decomposition of SOM to

446   decomposition of the added, more accessible substrate (Cheng, 1999; Kuzyakov, 2002).

447   These results are consistent with the theory that C availability is not limiting in highly

448   organic and less decomposed soils. Priming studies conducted in boreal, subarctic, and

449   permafrost regions that amended organic surface soils with glucose or low-molecular

450   weight C reported no net priming effects (Hartley et al., 2010; Lindén et al., 2014; Wild

451   et al., 2014; De Baets et al., 2016; Karhu et al., 2016; Rousk et al., 2016; Lynch et al.,

452   2018). Labile C addition to highly organic layers seem to shift microbial substrate

453   utilization to more N-rich compounds, which can reduce total SOM decomposition

454   (Rousk et al., 2016). Considering the entire soil profile, the 7-day cumulative response

455   ratio of respired soil C in the surface layer is very close to 1. The glucose effect on the

456   magnitude of soil C loss in the glucose treatment was negligible, and closely matched

457   rates in unamended surface samples. Meanwhile, positive priming in the permafrost

458   layer doubled the amount of C respired relative to permafrost unamended samples.

459   The strong negative priming response in surface soils during the 3rd cellulose pulse

460   may reflect the increasing C limitation of microorganisms during long-term incubations

461   (Bracho et al., 2016). Since 74-92% of the added cellulose remained in the soil after each

462   pulse, and $\delta^{13}CO_2$-C was still high 105 DAP, it is possible that microbes relied on the

463   accumulated cellulose as a source of C instead of SOM after almost one year of

464   incubation.

465   In the permafrost layer; the stimulation of daily CO_2-C production (7.66 to 28.67 µg

466   CO_2-C g^{-1}C) caused by the 3rd cellulose pulse was small compared to the initial microbial

467   biomass in the permafrost layer (660 ± 120 µg microbial C g^{-1}C). Thus, we cannot fully

468   attribute this positive priming effect in the cellulose treatment to higher SOM

469   decomposition, but potentially to an increase in microbial turnover (i.e. apparent

470   priming effect) (Jenkinson et al., 1985; Blagodatskaya and Kuzyakov, 2008). If we

471   consider the effect of cellulose addition on the entire soil profile, negative priming

472   effects in the surface were 2-5 times higher than positive priming effects in the

473   permafrost.

474   *4.2.   Persistent SOM decomposition response to multiple glucose additions*

475   Our results show that over the course of the incubation, each pulse of glucose

476   elicited a priming response. In the permafrost layer, glucose addition consistently

477   doubled soil C loss (Figure 2). Priming studies that repeatedly amended soils with

478   multiple pulses of substrate C have reported higher soil C losses than single additions at

479   the beginning of an incubation (De Nobili et al., 2001; Hamer and Marschner, 2005).

480   Glucose was readily used by microbes in the permafrost layer, and 68-126% of the

481   added substrate was completely respired 152 days following each pulse. Out of the

482   substrate respired, 20-47% was respired just in the first week, which is when we

483   observed positive priming effects. Glucose often produces a rapid response in microbial

484   activity (Bernal et al., 2016), and leads to rapid metabolic changes in a wide variety of

485   fast-growing bacteria that utilize it as a substrate (Stotzky and Norman, 1961; Hungate

486   et al., 2015). This fast turnover of glucose in permafrost soil, which can be seen in the

22

487 rapid decline in CO_2 flux and $\delta^{13}CO_2$-C (Supplemental Figures 1 and 2), and the sustained

488 positive priming effects over the course of the incubation suggest that multiple pulses

489 will continue to stimulate soil C loss, and single-pulse incubation studies might

490 underestimate soil C losses.

491 *4.3.   Age of respired soil C decreases with glucose input*

492   Carbon in deep soil layers is mostly old, and its longer mean residence time is due

493 to different biological, physical, and chemical stabilization processes; in permafrost, soil

494 C persistence may also be promoted by low rates of DOC inputs (Schimel et al., 1994;

495 Schuur et al., 2009; Czimczik and Welker, 2010; Walvoord and Kurylyk, 2016). Though a

496 previous study found that soluble C inputs increased the proportion of older CO_2-C

497 fluxes in boreal soils (Lindén et al., 2014), our results indicate that an input of glucose

498 decreased the age of soil respired C in transition and permafrost layers. Glucose

499 amendment induced soil C mineralization that was overall 115‰ higher (younger)

500 relative to soil C respired in unamended and cellulose treatments. Though other

501 permafrost priming studies do not report radiocarbon age of respired soil C, two priming

502 studies in other ecosystems also reported younger C losses. Blagodatskaya et al. (2011)

503 found that primed SOM decomposition originated mainly from younger C, even though

504 the proportion of young and old C equally contributed to SOM. Sullivan and Hart (2013)

505 conducted a priming experiment at four sites along a substrate age gradient from 0.93-

506 3000 ky, and found the greatest cumulative priming in younger sites, while the oldest

507 site experienced either negative or no net priming .

508   Recent arguments have been raised against the long-standing theory that

509   persistent soil C is found in large humic substances, but rather in a continuum of

510   progressively more decomposed compounds that transition from polymers to

511   monomers as OM is oxidized (Lehmann and Kleber, 2015). Older C fractions are not

512   always composed of complex or recalcitrant compounds (Kleber et al., 2011; Nunan et

513   al., 2015). Observations in a long-term bare-fallow soil that was depleted of plant litter

514   inputs showed that microbial communities became adapted to metabolizing simple and

515   small compounds. Microbes tended to use molecules or derivatives from the Krebs cycle

516   (i.e. α-ketoglutaric acid, citric acid), and were less able to decompose polymers, and

517   although old C molecules can be readily mineralized, the energetic payoff is low (Nunan

518   et al., 2015). The microbial mining hypothesis suggests that SOM decomposition

519   increases when microbes use extracellular enzymes to release nutrients locked in

520   polymers (Craine et al., 2007; Fontaine et al., 2011; Dijkstra et al., 2013). When a fresh C

521   substrate is introduced that increases microbial activity and extracellular enzyme

522   production, microbes can access C and nutrients in more complex polymeric structures.

523   If these complex C structures are younger, then positive priming may increase the

524   proportion of younger C that is respired. Soil C stabilization mechanisms in permafrost

525   are not completely understood, and in general, permafrost C is considered stable

526   primarily due to low temperature constraints on decomposition. Once temperature

527   constraints are lifted, mechanisms like waterlogging, microaggregation, and association

528   with silt and clay particles may also contribute to C stabilization (Six et al., 2002). Future

529   priming studies in permafrost should focus on physical stabilization processes that

530   influence C turnover rates.

531   A previous study at Eight Mile Lake found that the proportion of old C respired from

532   deeply thawed, experimentally warmed plots, was lower relative to less thawed areas.

533   They attributed this phenomenon to higher plant respiration, which increased the

534   contribution of younger C to ecosystem respiration and diluted the old C signature

535   (Schuur et al., 2009; Hicks Pries et al., 2015). Our results suggest that positive priming in

536   deep soil layers can also contribute to a younger signature of ecosystem respiration. The

537   average Δ^{14}C in unamended samples was -201‰ (CI: -296 to -110‰) in the transition

538   layer and -426‰ (CI: -516 to -334‰) in the permafrost layer. Priming increased the

539   respired Δ^{14}C values to -86‰ in the transition layer and -311‰ in the permafrost layer.

540   Though these values still reflect relatively older C, the change corresponds to potential

541    $\Delta^{14}CO_2$ that could be measured in layers that are 10-30 cm shallower than the depths

542   they originated from. Applying a partitioning model without considering priming effects

543   could cause the model to underestimate deep soil C contribution to ecosystem

544   respiration by attributing them to decomposition of shallower soils that have a greater

545   proportion of younger C.

546   *4.4.   Implications for permafrost-C feedback*

547   Our findings indicate that priming effects can have implications for the magnitude

548   and turnover of soil C in permafrost. Priming doubled permafrost soil C losses in the first

549   week after each pulse, and decreased the overall age of respired soil C. Field ecosystem

550   respiration measurements show that moist acidic tundra sites at Eight Mile Lake are a

551   net annual CO_2-C source to the atmosphere, despite increases in plant biomass (Mauritz

552   et al., 2017). This effect could be exacerbated by increased inputs of easily

553   decomposable C to mineral and permafrost soils. We extrapolated our incubation

554   results to field conditions at Eight Mile Lake by using field soil temperatures to

555   temperature-correct soil C fluxes, and applied a site specific Q_{10} of 2.6 based on the

556   temperature sensitivity analysis of CO_2 fluxes from soils collected in our site in 2010

557   (Bracho et al., 2016). Our estimates suggest that priming-induced soil C losses

558   correspond to 4-12% of the cumulative C released during a growing season (235 - 408 g

559   CO_2-C m^{-2}, reported in Mauritz et al. 2017). Though we must be cautious when relating

560   incubation results to the field, as these estimates are likely high because soils can

561   remain waterlogged after thaw, and our sample size is small, our study suggests that

562   priming may be an important mechanism that exacerbates soil C losses to the

563   atmosphere. Future priming studies should focus on field studies, and measure the

564   radiocarbon age of primed soil C. We must consider priming effects to fully understand

565   permafrost C dynamics, or we may potentially underestimate the contribution of soil C

566   to ecosystem respiration rates.

26

567 **Acknowledgements**

574   Alewell, C., Giesler, R., Klaminder, J., Leifeld, J., Rollog, M., 2011. Stable carbon
575   isotopes as indicators for environmental change in palsa peats. Biogeosciences 8, 1769-
576   1778 doi: 10.5194/bg-8-1769-2011.

577   Baldock, J.A., Skjemstad, J.O., 2000. Role of the soil matrix and minerals in protecting
578   natural organic materials against biological attack. Organic Geochemistry 31, 697-710
579   doi: 10.1016/S0146-6380(00)00049-8.

580   Bates, D., Machler, M., Bolker, B.M., Walker, S.C., 2015. Fitting linear mixed-effects
581   models using lme4. Journal of Statistical Software 67, 1-48 doi: 10.18637/jss.v067.i01.

582   Bauer, J.E., Williams, P.M., Druffel, E.R.M., 1992. Recovery of submilligram quantities
583   of carbon-dioxide from gas streams by molecular-sieve for subsequent determination of
584   isotopic (C-13 and C-14) natural abundances. Analytical Chemistry 64, 824-827 doi:
585   10.1021/ac00031a024.

586   Bernal, B., McKinley, D.C., Hungate, B.A., White, P.M., Mozdzer, T.J., Megonigal, J.P.,
587   2016. Limits to soil carbon stability; Deep, ancient soil carbon decomposition stimulated
588   by new labile organic inputs. Soil Biology & Biochemistry 98, 85-94 doi:
589   10.1016/j.soilbio.2016.04.007.

590   Bingeman, C.W., Varner, J.E., Martin, W.P., 1953. The effect of the addition of organic
591   materials on the decomposition of an organic soil. Soil Sci. Soc. Am. J. 17, 34-38 doi:
592   10.2136/sssaj1953.03615995001700010008x.

593   Blagodatskaya, E., Kuzyakov, Y., 2008. Mechanisms of real and apparent priming effects
594   and their dependence on soil microbial biomass and community structure: critical review.
595   Biology and Fertility of Soils 45, 115-131 doi: 10.1007/S00374-008-0334-Y.

596   Blagodatskaya, E., Yuyukina, T., Blagodatsky, S., Kuzyakov, Y., 2011. Three-source-
597   partitioning of microbial biomass and of CO2 efflux from soil to evaluate mechanisms of
598   priming effects. Soil Biology & Biochemistry 43, 778-786 doi:
599   10.1016/j.soilbio.2010.12.011.

600   Bracho, R., Natali, S., Pegoraro, E., Crummer, K.G., Schädel, C., Celis, G., Hale, L., Wu,
601   L.Y., Yin, H.Q., Tiedje, J.M., Konstantinidis, K.T., Luo, Y.Q., Zhou, J.Z., Schuur,
602   E.A.G., 2016. Temperature sensitivity of organic matter decomposition of permafrost-
603   region soils during laboratory incubations. Soil Biology & Biochemistry 97, 1-14 doi:
604   10.1016/j.soilbio.2016.02.008.

605   Brown, J., Romanovsky, V.E., 2008. Report from the International Permafrost
606   Association: State of permafrost in the first decade of the 21(st) century. Permafrost and
607   Periglacial Processes 19, 255-260 doi: Doi 10.1002/Ppp.618.

608 Chapin, F.S., Shaver, G.R., Giblin, A.E., Nadelhoffer, K.J., Laundre, J.A., 1995.
609 Responses of Arctic tundra to experimental and observed changes in climate. Ecology 76,
610 694-711 doi: 10.2307/1939337.

611 Cheng, W.X., 1999. Rhizosphere feedbacks in elevated CO2. Tree Physiology 19, 313-
612 320 doi: 10.1093/treephys/19.4-5.313.

613 Craine, J.M., Morrow, C., Fierer, N., 2007. Microbial nitrogen limitation increases
614 decomposition. Ecology 88, 2105-2113 doi: 10.1890/06-1847.1.

615 Czimczik, C.I., Welker, J.M., 2010. Radiocarbon content of CO2 respired from high
616 Arctic tundra in Northwest Greenland. Arctic Antarctic and Alpine Research 42, 342-350
617 doi: 10.1657/1938-4246-42.3.342.

618 De Baets, S., van de Weg, M.J., Lewis, R., Steinberg, N., Meersmans, J., Quine, T.A.,
619 Shaver, G.R., Hartley, I.P., 2016. Investigating the controls on soil organic matter
620 decomposition in tussock tundra soil and permafrost after fire. Soil Biology &
621 Biochemistry 99, 108-116 doi: 10.1016/j.soilbio.2016.04.020.

622 De Nobili, M., Contin, M., Mondini, C., Brookes, P.C., 2001. Soil microbial biomass is
623 triggered into activity by trace amounts of substrate. Soil Biology & Biochemistry 33,
624 1163-1170 doi: 10.1016/S0038-0717(01)00020-7.

625 Deane-Coe, K.K., Mauritz, M., Celis, G., Salmon, V.G., Crummer, K.G., Natali, S.M.,
626 Schuur, E.A.G., 2015. Experimental warming alters productivity and isotopic signatures
627 of tundra mosses. Ecosystems 18, 1070-1082 doi: 10.1007/s10021-015-9884-7.

628 Derrien, D., Marol, C., Balesdent, J., 2004. The dynamics of neutral sugars in the
629 rhizosphere of wheat. An approach by C-13 pulse-labelling and GC/C/IRMS. Plant and
630 Soil 267, 243-253 doi: 10.1007/s11104-005-5348-8.

631 Dijkstra, F.A., Carrillo, Y., Pendall, E., Morgan, J.A., 2013. Rhizosphere priming: a
632 nutrient perspective. Frontiers in Microbiology 4 doi: 10.3389/fmicb.2013.00216.

633 Dutta, K., Schuur, E.A.G., Neff, J.C., Zimov, S.A., 2006. Potential carbon release from
634 permafrost soils of Northeastern Siberia. Global Change Biology 12, 2336-2351 doi:
635 10.1111/j.1365-2486.2006.01259.x.

636 Fan, Z., Jastrow, J.D., Liang, C., Matamala, R., Miller, R.M., 2013. Priming effects in
637 boreal black spruce forest soils: Quantitative evaluation and sensitivity analysis. Plos one
638 8 doi: 10.1371/journal.pone.0077880.

29

639 Fontaine, S., Barot, S., Barre, P., Bdioui, N., Mary, B., Rumpel, C., 2007. Stability of
640 organic carbon in deep soil layers controlled by fresh carbon supply. Nature 450, 277–
641 280 doi: 10.1038/nature06275.

642 Fontaine, S., Henault, C., Aamor, A., Bdioui, N., Bloor, J.M.G., Maire, V., Mary, B.,
643 Revaillot, S., Maron, P.A., 2011. Fungi mediate long term sequestration of carbon and
644 nitrogen in soil through their priming effect. Soil Biology & Biochemistry 43, 86-96 doi:
645 10.1016/j.soilbio.2010.09.017.

646 Hamer, U., Marschner, B., 2005. Priming effects in soils after combined and repeated
647 substrate additions. Geoderma 128, 38-51 doi: 10.1016/j.geoderma.2004.12.014.

648 Harden, J., Koven, C., Ping, C., Hugelius, G., McGuire, A., Camill, P., Jorgenson, T.,
649 Kuhry, P., Michaelson, G., O'Donnell, J., Schuur, E., Tarnocai, C., Johnson, K., Grosse,
650 G., 2012. Field information links permafrost carbon to physical vulnerabilities of
651 thawing. Geophysical Research Letters 39 doi: 10.1029/2012GL051958.

652 Hardie, S.M.L., Garnett, M.H., Fallick, A.E., Rowland, A.P., Ostle, N.J., 2005. Carbon
653 dioxide capture using a zeolite molecular sieve sampling system for isotopic studies (C-
654 13 and C-14) of respiration. Radiocarbon 47, 441-451 doi: 10.1017/S0033822200035220.

655 Hartley, I.P., Hopkins, D.W., Sommerkorn, M., Wookey, P.A., 2010. The response of
656 organic matter mineralisation to nutrient and substrate additions in sub-arctic soils. Soil
657 Biology & Biochemistry 42, 92-100 doi: 10.1016/j.soilbio.2009.10.004.

658 Hicks Pries, Caitlin E., Schuur, E.A.G., Natali, Susan M., Crummer, K.G., 2015. Old soil
659 carbon losses increase with ecosystem respiration in experimentally thawed tundra.
660 Nature Climate Change 6, 214-218 doi: 10.1038/nclimate2830.

661 Hugelius, G., Strauss, J., Zubrzycki, S., Harden, J.W., Schuur, E.A.G., Ping, C.L.,
662 Schirrmeister, L., Grosse, G., Michaelson, G.J., Koven, C., O´Donnell, J., Elberling, B.,
663 Mishra, U., Camill, P., Yu, Z., Palmtag, J., Kuhry, P., 2014. Estimated stocks of
664 circumpolar permafrost carbon with quantified uncertainty ranges and identified data
665 gaps. Biogeosciences 11, 6573-6593 doi: 10.5194/bg-11-6573-2014.

666 Hungate, B.A., Mau, R.L., Schwartz, E., Caporaso, J.G., Dijkstra, P., van Gestel, N.,
667 Koch, B.J., Liu, C.M., McHugh, T.A., Marks, J.C., Morrissey, E.M., Price, L.B., 2015.
668 Quantitative microbial ecology through stable isotope probing. Applied and
669 Environmental Microbiology 81, 7570-7581 doi: 10.1128/Aem.02280-15.

670 IPCC, 2013. Climate Change 2013: The physical science basis. Contribution of working
671 group I to the fifth assessment report of the Intergovernmental Panel on Climate Change.
672 Cambridge University Press, Cambridge, United Kingdom and New York, NY, USA.

673 Jenkinson, D.S., Fox, R.H., Rayner, J.H., 1985. Interactions between fertilizer nitrogen
674 and soil nitrogen−the so‐called 'priming' effect. Journal of Soil Science 36, 425-444
675 doi: 10.1111/j.1365-2389.1985.tb00348.x.

676 Karhu, K., Hilasvuori, E., Fritze, H., Biasi, C., Nykanen, H., Liski, J., Vanhala, P.,
677 Heinonsalo, J., Pumpanen, J., 2016. Priming effect increases with depth in a boreal forest
678 soil. Soil Biology & Biochemistry 99, 104-107 doi: 10.1016/j.soilbio.2016.05.001.

679 Keuper, F., Dorrepaal, E., van Bodegom, P.M., van Logtestijn, R., Venhuizen, G., van
680 Hal, J., Aerts, R., 2017. Experimentally increased nutrient availability at the permafrost
681 thaw front selectively enhances biomass production of deep-rooting subarctic peatland
682 species. Global Change Biology 23, 4257-4266 doi: 10.1111/gcb.13804.

683 Keuper, F., van Bodegom, P.M., Dorrepaal, E., Weedon, J.T., van Hal, J., van Logtestijn,
684 R.S.P., Aerts, R., 2012. A frozen feast: thawing permafrost increases plant-available
685 nitrogen in subarctic peatlands. Global Change Biology 18 doi: 10.1111/j.1365-
686 2486.2012.02663. x.

687 Kleber, M., Nico, P.S., Plante, A.F., Filley, T., Kramer, M., Swanston, C., Sollins, P.,
688 2011. Old and stable soil organic matter is not necessarily chemically recalcitrant:
689 implications for modeling concepts and temperature sensitivity. Global Change Biology
690 17, 1097-1107 doi: 10.1111/j.1365-2486.2010.02278.x.

691 Knoblauch, C., Beer, C., Sosnin, A., Wagner, D., Pfeiffer, E.M., 2013. Predicting long-
692 term carbon mineralization and trace gas production from thawing permafrost of
693 Northeast Siberia. Global Change Biology 19, 1160-1172 doi: 10.1111/gcb.12116.

694 Kögel-Knabner, I., 2002. The macromolecular organic composition of plant and
695 microbial residues as inputs to soil organic matter. Soil Biology & Biochemistry 34, 139-
696 162 doi: 10.1016/s0038-0717(01)00158-4.

697 Kuzyakov, Y., 2002. Review: Factors affecting rhizosphere priming effects. Journal of
698 Plant Nutrition and Soil Science 165, 382-396 doi: 10.1002/1522-
699 2624(200208)165:4<382::Aid-Jpln382>3.0.Co;2-#.

700 Lehmann, J., Kleber, M., 2015. The contentious nature of soil organic matter. Nature 528,
701 60-68 doi: 10.1038/nature16069.

702 Lindén, A., Heinonsalo, J., Buchmann, N., Oinonen, M., Sonninen, E., Hilasvuori, E.,
703 Pumpanen, J., 2014. Contrasting effects of increased carbon input on boreal SOM
704 decomposition with and without presence of living root system of Pinus sylvestris L.
705 Plant and Soil 377, 145-158 doi: 10.1007/s11104-013-1987-3.

706 Lynch, L.M., Machmuller, M.B., Cotrufo, M.F., Paul, E.A., Wallenstein, M.D., 2018.
707 Tracking the fate of fresh carbon in the Arctic tundra: Will shrub expansion alter
708 responses of soil organic matter to warming? Soil Biology & Biochemistry 120, 134-144
709 doi: 10.1016/j.soilbio.2018.02.002.

710 Mau, R.L., Liu, C.M., Aziz, M., Schwartz, E., Dijkstra, P., Marks, J.C., Price, L.B.,
711 Keim, P., Hungate, B.A., 2015. Linking soil bacterial biodiversity and soil carbon
712 stability. ISME 9, 1477, 1480 doi: 10.1038/ismej.2014.205.

713 Mauritz, M., Bracho, R., Celis, G., Hutchings, J., Natali, S.M., Pegoraro, E., Salmon,
714 V.G., Schädel, C., Webb, E.E., Schuur, E.A.G., 2017. Non-linear CO2 flux response to
715 seven years of experimentally induced permafrost thaw. Global Change Biology doi:
716 10.1111/gcb.13661

717 Natali, S., Schuur, E., Rubin, R., 2012. Increased plant productivity in Alaskan tundra as
718 a result of experimental warming of soil and permafrost. Journal of Ecology 100, 488-
719 498 doi: 10.1111/j.1365-2745.2011.01925.x.

720 Natali, S., Schuur, E., Trucco, C., Pries, C., Crummer, K., Lopez, A., 2011. Effects of
721 experimental warming of air, soil and permafrost on carbon balance in Alaskan tundra.
722 Global Change Biology 17, 1394-1407 doi: 10.1111/j.1365-2486.2010.02303.x.

723 Nowinski, N.S., Taneva, L., Trumbore, S.E., Welker, J.M., 2010. Decomposition of old
724 organic matter as a result of deeper active layers in a snow depth manipulation
725 experiment. Oecologia 163, 785–792 doi: 10.1007/s00442-009-1556-x.

726 Nunan, N., Lerch, T.Z., Pouteau, V., Mora, P., Changey, E., Katterer, T., Giusti-Miller,
727 S., Herrmann, A.M., 2015. Metabolising old soil carbon: Simply a matter of simple
728 organic matter? Soil Biology & Biochemistry 88, 128-136 doi:
729 10.1016/j.soilbio.2015.05.018.

730 Osterkamp, T.E., Jorgenson, M.T., Schuur, E.A.G., Shur, Y.L., Kanevskiy, M.Z., Vogel,
731 J.G., Tumskoy, V.E., 2009. Physical and ecological changes associated with warming
732 permafrost and thermokarst in interior Alaska. Permafrost and Periglacial Processes 20,
733 235-256 doi: 10.1002/ppp.656.

734 Paterson, E., Midwood, A.J., Millard, P., 2009. Through the eye of the needle: a review
735 of isotope approaches to quantify microbial processes mediating soil carbon balance.
736 New Phytologist 184, 19-33 doi: Doi 10.1111/J.1469-8137.2009.03001.X.

737 Plaza, C., Schuur, E.A.G., Pegoraro, E.F., 2017a. Eight Mile Lake research watershed,
738 Carbon in Permafrost Experimental Heating Research (CiPEHR): nuclear magnetic
739 resonance spectra of soils, 2009 and 2013, LTER Bonanza Creek.

740 Plaza, C., Schuur, E.A.G., Pegoraro, E.F., 2017b. Eight Mile Lake research watershed,
741 Carbon in Permafrost Experimental Heating Research (CiPEHR): physical and chemical
742 properties of soils, 2009-2013, LTER Bonanza Creek.

743 Pries, C.E.H., Schuur, E.A.G., Crummer, K.G., 2012. Holocene carbon stocks and carbon
744 accumulation rates altered in soils undergoing permafrost thaw. Ecosystems 15, 162-173
745 doi: 10.1007/s10021-011-9500-4.

746 R Development Core Team, 2015. R: A language and environment for statistical
747 computing. R Foundation for Statistical Computing, Vienna, Austria.

748 Romanovsky, V., Smith, S., Christiansen, H., 2010. Permafrost thermal state in the polar
749 Northern Hemisphere during the international polar year 2007-2009: a synthesis.
750 Permafrost and Periglacial Processes 21, 106-116 doi: 10.1002/ppp.689.

751 Romanovsky, V.E., Smith, S.L., Christiansen, H.H., Shiklomanov, N.I., Streletskiy, D.A.,
752 Drozdov, D.S., Oberman, N.G., Kholodov, A.L., Marchenko, S.S., 2012. Permafrost [in
753 Arctic Report Card 2012]. NOAA.

754 Rousk, K., Michelsen, A., Rousk, J., 2016. Microbial control of soil organic matter
755 mineralization responses to labile carbon in subarctic climate change treatments. Global
756 Change Biology 22, 4150-4161 doi: 10.1111/gcb.13296.

757 Rustad, L., Campbell, J., Marion, G., Norby, R., Mitchell, M., Hartley, A., Cornelissen,
758 J., Gurevitch, J., Gcte, N., 2001. A meta-analysis of the response of soil respiration, net
759 nitrogen mineralization, and aboveground plant growth to experimental ecosystem
760 warming. Oecologia 126, 543-562 doi: 10.1007/s004420000544.

761 Salmon, V.G., Schädel, C., Bracho, R., Pegoraro, E., Celis, G., Mauritz, M., Mack, M.C.,
762 Schuur, E.A.G., 2018. Adding depth to our understanding of nitrogen dynamics in
763 permafrost soils. Journal of Geophysical Research: Biogeosciences 123 doi:
764 10.1029/2018JG004518.

765 Schädel, C., Luo, Y.Q., Evans, R.D., Fei, S.F., Schaeffer, S.M., 2013. Separating soil
766 CO_2 efflux into C-pool-specific decay rates via inverse analysis of soil incubation data.
767 Oecologia 171, 721-732 doi: 10.1007/s00442-012-2577-4.

768 Schädel, C., Schuur, E.A.G., Bracho, R., Elberling, B., Knoblauch, C., Lee, H., Luo,
769 Y.Q., Shaver, G.R., Turetsky, M.R., 2014. Circumpolar assessment of permafrost C
770 quality and its vulnerability over time using long-term incubation data. Global Change
771 Biology 20, 641-652 doi: 10.1111/gcb.12417

772 Schimel, D.S., Braswell, B.H., Holland, E.A., Mckeown, R., Ojima, D.S., Painter, T.H.,
773 Parton, W.J., Townsend, A.R., 1994. Climatic, edaphic, and biotic controls over storage
774 and turnover of carbon in soils. Global Biogeochemical Cycles 8, 279-293 doi:
775 10.1029/94gb00993.

776 Schimel, J.P., Weintraub, M.N., 2003. The implications of exoenzyme activity on
777 microbial carbon and nitrogen limitation in soil: A theoretical model. Soil Biology &
778 Biochemistry 35, 549-563 doi: 10.1016/S0038-0717(03)00015-4.

779 Schuur, E.A.G., Bockheim, J., Canadell, J.G., Euskirchen, E., Field, C.B., Goryachkin,
780 S.V., Hagemann, S., Kuhry, P., Lafleur, P.M., Lee, H., Mazhitova, G., Nelson, F.E.,
781 Rinke, A., Romanovsky, V.E., Shiklomanov, N., Tarnocai, C., Venevsky, S., Vogel, J.G.,
782 Zimov, S.A., 2008. Vulnerability of permafrost carbon to climate change: Implications
783 for the global carbon cycle. Bioscience 58, 701-714 doi: 10.1641/B580807.

784 Schuur, E.A.G., Crummer, K.G., Vogel, J.G., Mack, M.C., 2007. Plant species
785 composition and productivity following permafrost thaw and thermokarst in alaskan
786 tundra. Ecosystems 10, 280-292 doi: 10.1007/s10021-007-9024-0.

787 Schuur, E.A.G., McGuire, A.D., Schädel, C., Grosse, G., Harden, J.W., Hayes, D.J.,
788 Hugelius, G., Koven, C.D., Kuhry, P., Lawrence, D.M., Natali, S.M., Olefeldt, D.,
789 Romanovsky, V.E., Schaefer, K., Turetsky, M.R., Treat, C.C., Vonk, J.E., 2015. Climate
790 change and the permafrost carbon feedback. Nature 520, 171-179 doi:
791 10.0.4.14/nature14338.

792 Schuur, E.A.G., Trumbore, S.E., 2006. Partitioning sources of soil respiration in boreal
793 black spruce forest using radiocarbon. Global Change Biology 12, 165-176 doi:
794 10.1111/j.1365-2486.2005.01066.x

795 Schuur, E.A.G., Vogel, J.G., Crummer, K.G., Lee, H., Sickman, J.O., Osterkamp, T.E.,
796 2009. The effect of permafrost thaw on old carbon release and net carbon exchange from
797 tundra. Nature 459, 556-559 doi: 10.1038/nature08031.

798 Shaver, G.R., Canadell, J., Chapin, F.S., Gurevitch, J., Harte, J., Henry, G., Ineson, P.,
799 Jonasson, S., Melillo, J., Pitelka, L., Rustad, L., 2000. Global warming and terrestrial
800 ecosystems: A conceptual framework for analysis. Bioscience 50, 871-882 doi:
801 10.1641/0006-3568(2000)050[0871:GWATEA]2.0.CO;2.

802 Six, J., Conant, R.T., Paul, E.A., Paustian, K., 2002. Stabilization mechanisms of soil
803 organic matter: Implications for C-saturation of soils. Plant and Soil 241, 155-176 doi:
804 10.1023/A:1016125726789.

805 Soil Survey Staff, 2014. Keys to Soil Taxonomy 12 ed. USDA-Natural Resources
806 Conservation Service, Washington, DC.

807 Stotzky, G., Norman, A.G., 1961. Factors limiting microbial activities in soil. Archiv.
808 Mikrobiol. 40, 370-382 doi: 10.1007/Bf00422051.

809 Stuiver, M., Polach, H.A., 1977. Discussion: reporting of 14C data. Radiocarbon 19, 355-
810 363 doi: 10.1017/S0033822200003672.

811 Sullivan, B.W., Hart, S.C., 2013. Evaluation of mechanisms controlling the priming of
812 soil carbon along a substrate age gradient. Soil Biology & Biochemistry 58, 293-301 doi:
813 10.1016/j.soilbio.2012.12.007.

814 Sullivan, P.F., Sommerkorn, M., Rueth, H.M., Nadelhoffer, K.J., Shaver, G.R., Welker,
815 J.M., 2007. Climate and species affect fine root production with long-term fertilization in
816 acidic tussock tundra near Toolik Lake, Alaska. Oecologia 153, 643-652 doi:
817 10.1007/s00442-007-0753-8.

818 Tape, K., Sturm, M., Racine, C., 2006. The evidence for shrub expansion in Northern
819 Alaska and the Pan-Arctic. Global Change Biology 12, 686-702 doi: 10.1111/j.1365-
820 2486.2006.01128.x.

821 Tarnocai, C., Canadell, J.G., Schuur, E., Kuhry, P., Mazhitova, G., Zimov, S., 2009. Soil
822 organic carbon pools in the northern circumpolar permafrost region. Global
823 Biogeochemical Cycles 23 doi: 10.1029/2008GB003327.

824 Torn, M.S., Southon, J.R., 2001. A new 13C correction for radiocarbon samples from
825 elevated-CO2 experiments. Radiocarbon 43, 691-694.

826 Trumbore, S., 2000. Age of soil organic matter and soil respiration: Radiocarbon
827 constraints on belowground C dynamics. Ecological Applications 10, 399-411 doi:
828 10.1890/1051-0761(2000)010[0399:Aosoma]2.0.Co;2.

829 Trumbore, S.E., Sierra, C.A., Hicks Pries, C.E., 2016a. Radiocarbon nomenclature,
830 theory, models, and interpretation: Measuring age, determining cycling rates, and tracing
831 source pools, In: Schuur, E.A.G., Druffel, E.R.M., Trumbore, S.E. (Eds.), Radiocarbon
832 and Climate Change. Springer, pp. 45-82.

833 Trumbore, S.E., Xu, X., Santos, G.M., Czimczik, C.I., Beaupre, S.R., Pack, M.A.,
834 Hopkins, F.M., Stills, A., Lupascu, M., Ziolkowski, L., 2016b. Preparation for
835 radiocarbon analysis, In: Schuur, E.A.G., Druffel, E.R.M., Trumbore, S.E. (Eds.),
836 Radiocarbon and Climate Change. Springer, pp. 279-308.

837 Turnbull, J.C., Graven, H., Krakauer, N.Y., 2016. Radiocarbon in the atmosphere, In:
838 Schuur, E.A.G., Druffel, E.R.M., Trumbore, S. (Eds.), Radiocarbon and Climate Change.
839 Springer, pp. 83-138.

840 Vogel, J.S., Nelson, D.E., Southon, J.R., 1987. C-14 background levels in an accelerator
841 mass-spectrometry system. Radiocarbon 29, 323-333 doi: 10.1017/S0033822200043733.

842 Vonk, J.E., Mann, P.J., Davydov, S., Davydova, A., Spencer, R.G.M., Schade, J.,
843 Sobczak, W.V., Zimov, N., Zimov, S., Bulygina, E., Eglinton, T.I., Holmes, R.M., 2013.
844 High biolability of ancient permafrost carbon upon thaw. Geophysical Research Letters
845 40, 2689-2693 doi: 10.1002/grl.50348.

846 Walvoord, M.A., Kurylyk, B.L., 2016. Hydrologic impacts of thawing permafrost—A
847 review. Vadose Zone Journal 15 doi: 10.2136/vzj2016.01.0010.

848 Wild, B., Gentsch, N., Capek, P., Diakova, K., Alves, R.J.E., Barta, J., Gittel, A.,
849 Hugelius, G., Knoltsch, A., Kuhry, P., Lashchinskiy, N., Mikutta, R., Palmtag, J.,
850 Schleper, C., Schnecker, J., Shibistova, O., Takriti, M., Torsvik, V.L., Urich, T., Watzka,
851 M., Santruckova, H., Guggenberger, G., Richter, A., 2016. Plant-derived compounds
852 stimulate the decomposition of organic matter in arctic permafrost soils. Scientific
853 Reports 6 doi: 10.0.4.14/srep25607.

854 Wild, B., Schnecker, J., Alves, R.J.E., Barsukov, P., Barta, J., Capek, P., Gentsch, N.,
855 Gittel, A., Guggenberger, G., Lashchinskiy, N., Mikutta, R., Rusalimova, O.,
856 Santruckova, H., Shibistova, O., Urich, T., Watzka, M., Zrazhevskaya, G., Richter, A.,
857 2014. Input of easily available organic C and N stimulates microbial decomposition of
858 soil organic matter in arctic permafrost soil. Soil Biology & Biochemistry 75, 143-151
859 doi: 10.1016/J.Soilbio.2014.04.014.

860 Zamin, T.J., Bret-Harte, M.S., Grogan, P., 2014. Evergreen shrubs dominate responses to
861 experimental summer warming and fertilization in Canadian mesic low arctic tundra.
862 Journal of Ecology 102, 749-766 doi: 10.1111/1365-2745.12237.

863 Zimov, S.A., Schuur, E.A.G., Chapin, F.S., 2006. Permafrost and the global carbon
864 budget. Science 312, 1612-1613 doi: 10.1126/science.1128908.
865

866 Table 1. Initial soil properties (mean ± SE) grouped by soil layers. A linear mixed effects model tested the effect of soil layer on bulk density,
867 initial bulk soil organic carbon and nitrogen (%), C:N, initial δ^{13}C (‰), microbial biomass, and pH. Values not sharing the same letter indicate a
868 significant difference.

Layer	Bulk Density (g/cm3)	Initial C (%)	Initial N (%)	C:N	Initial δ^{13}C (‰)	Microbial biomass (mg C g^{-1} soil C)	pH
Surface	0.17 ± 0.04[a]	37.96 ± 2.52[a]	1.51 ± 0.11[a]	25.52 ± 2.59[a]	-26.22 ± 0.17[a]	1.22 ± 0.76[a]	3.96 ± 0.09[a]
Transition	0.53 ± 0.15[b]	20.99 ± 3.92[b]	0.86 ± 0.20[b]	25.08 ± 1.88[a]	-27.22 ± 0.19[b]	0.36 ± 0.13[a]	4.77 ± 0.13[b]
Permafrost	0.46 ± 0.03[b]	9.69 ± 3.68[c]	0.37 ± 0.13[c]	24.80 ± 1.50[a]	-27.36 ± 0.23[b]	0.66 ± 0.12[a]	5.12 ± 0.15[c]
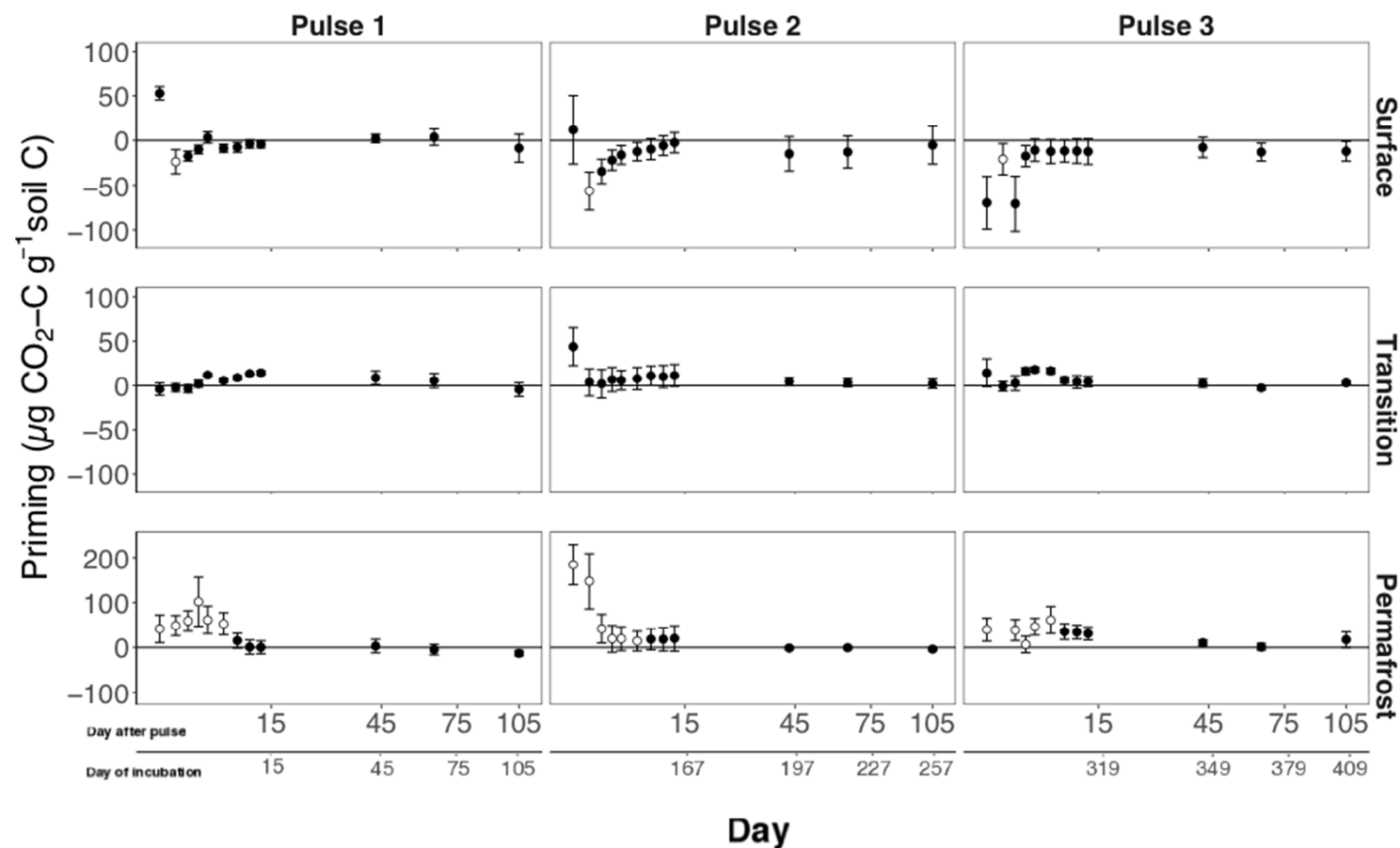
Figure 1. Priming (μg CO_2-C $g^{-1}C$) in surface, transition, and permafrost layers over time (in days) after glucose pulse amendment (DAP) (primary x-axis). The secondary x-axis indicates day since the start of incubation (DOI). The x-axis was square-root transformed to make it easier to see values in the first 15 DAP. Values above zero indicate higher soil C losses relative to control (positive priming), and values below zero indicate lower soil C losses relative to control (negative priming). Bars are one standard error from the mean, and open circles indicate a significant priming effect. Note that the scale for the y-axis in the permafrost layer is two times higher.

Cumulative response ratio of respired soil C after 7 days
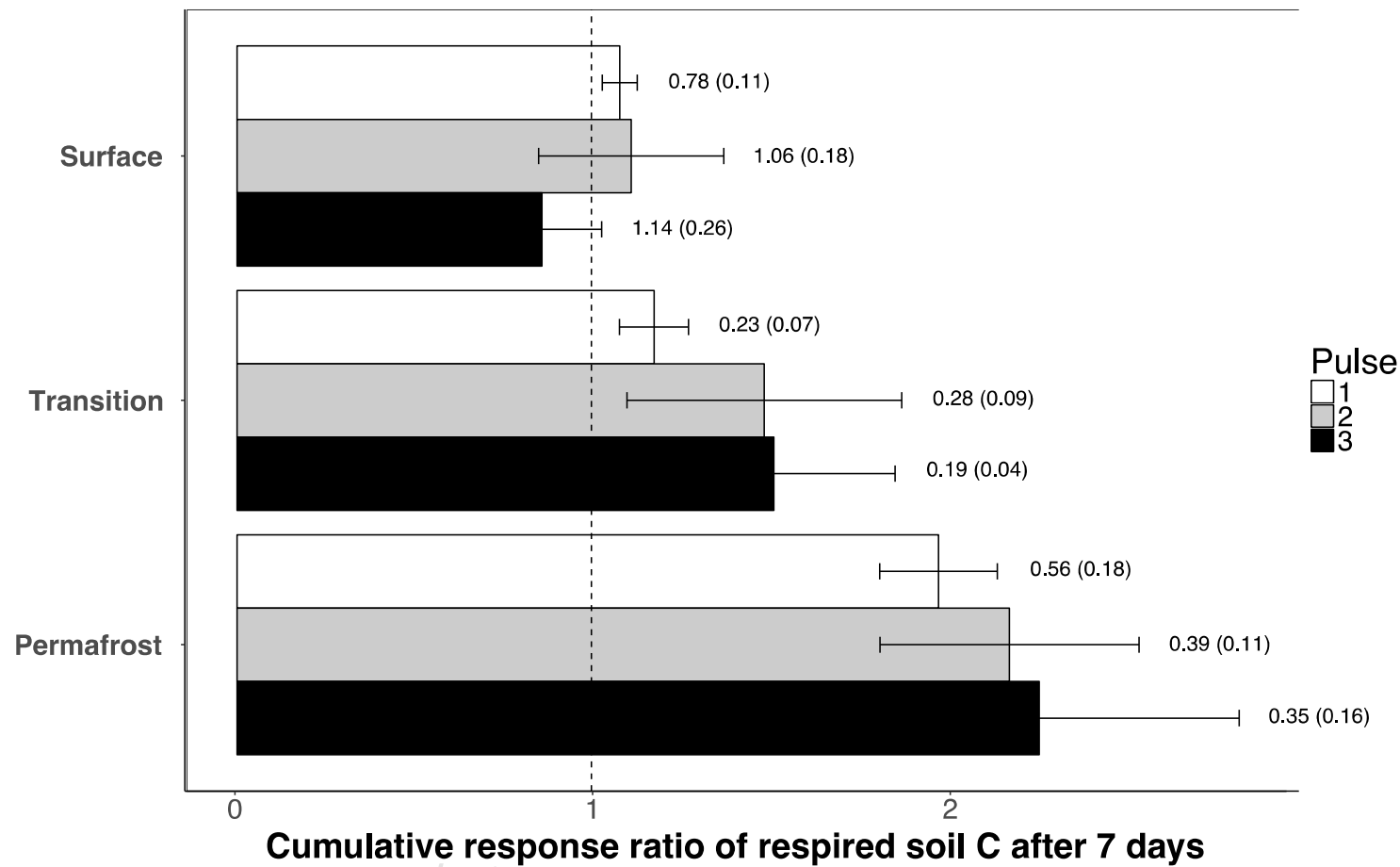
875
876
877 Figure 2. Cumulative response ratio of respired soil C in glucose treatments relative to respired soil C in unamended samples over 7 DAP. Glucose
878 to unamended ratios that are less than 1 indicate negative priming, equal to 1 indicate no priming effect, greater than 1 indicate positive
879 priming. Numbers in the figure are the unamended cumulative soil C losses (mg soil C g^{-1}C ± SE) 7 days after each pulse. Bars are one standard
880 error from the mean.
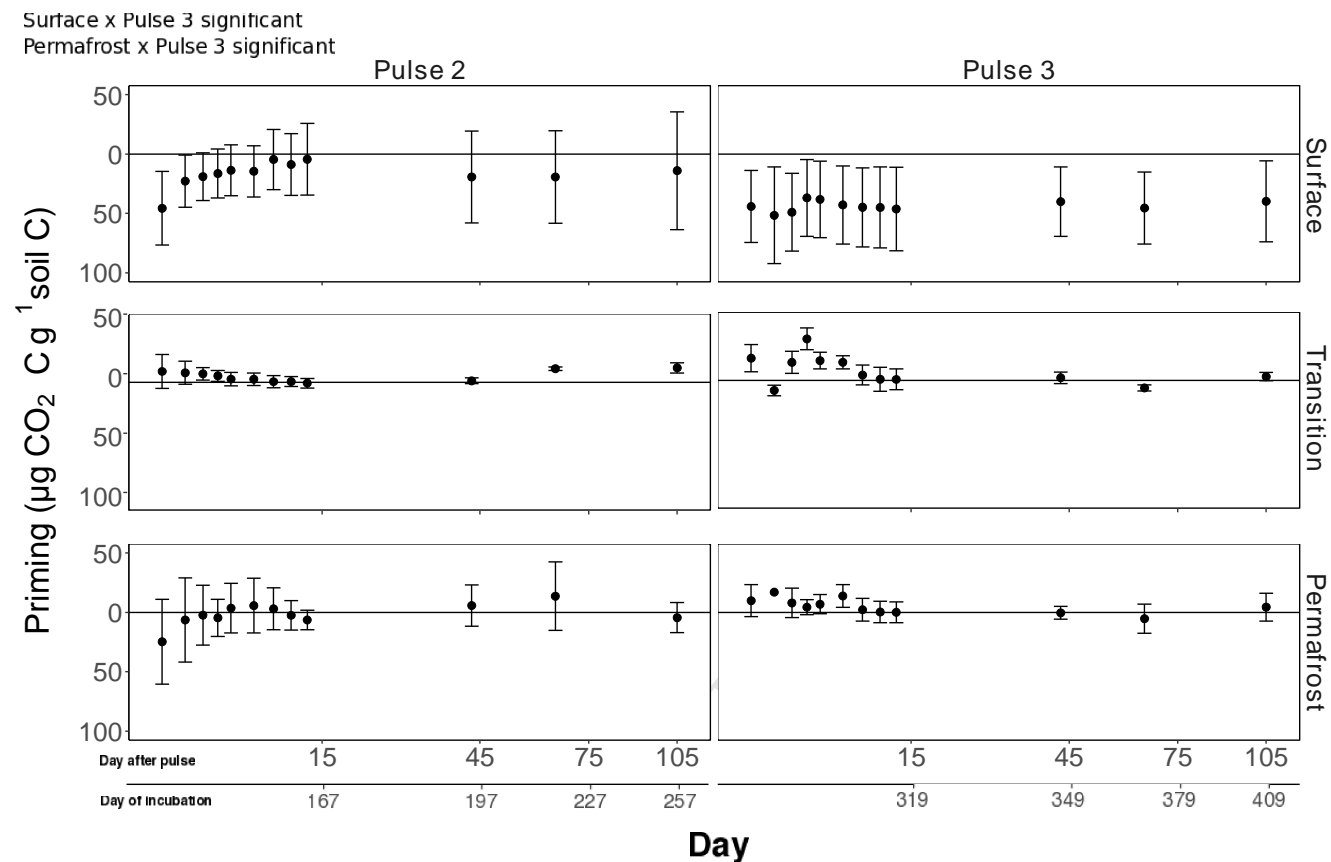
881
882 Figure 3. Priming (μg CO_2-C g^{-1}C) in surface, transition, and permafrost layers over time (in days) after cellulose pulse amendment (DAP) (primary
883 x-axis). The secondary x-axis indicates day since the start of incubation (DOI). The x-axis was square-root transformed to make it easier to see
884 values in the first 15 DAP. Labelling was not high enough in Pulse 1 to calculate priming effects (data not shown). Values above zero indicate
885 higher soil C losses relative to control (positive priming), and values below zero indicate lower soil C losses relative to control (negative priming).
886 Bars are one standard error from the mean. Surface and permafrost layers had significantly negative and positive priming, respectively, in Pulse
887 3.

888
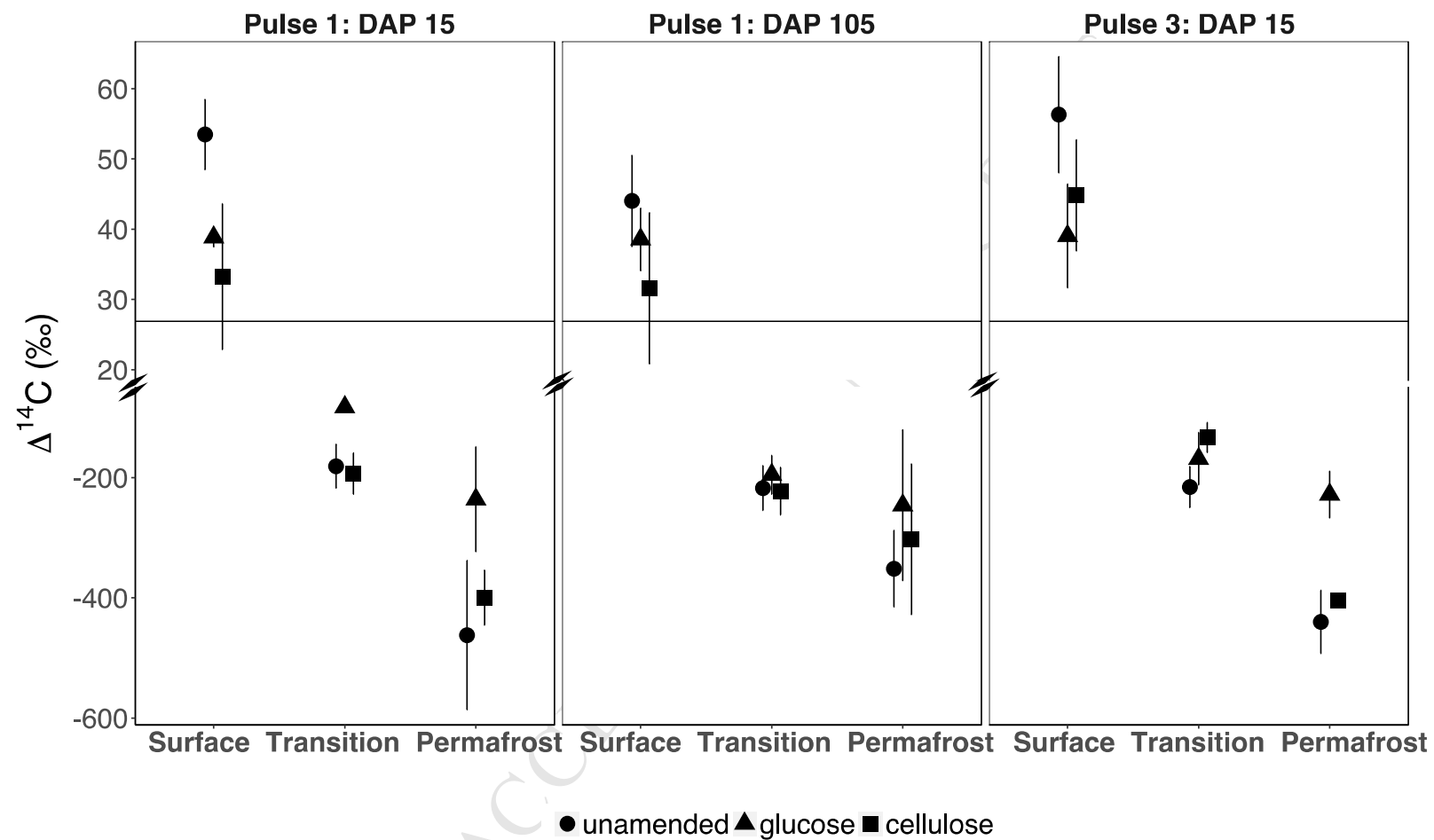
Figure 4. Mean soil respired Δ^{14}C (‰) in surface, transition, and permafrost layers by treatment 15 and 105 days after pulse 1, and 15 days after pulse 3 (DOI 319). Bars are one standard error from the mean. Horizontal line indicates atmospheric Δ^{14}C concentration in 2013. Note the break in the y-axis.

893 Table 2. Mixed linear effects model for soil respired Δ^{14}C at 15 and 105 days after the 1st amendment pulse, and DOI 319 (15 days after the 3rd
894 amendment pulse). The intercept for the surface model represents soil respired Δ^{14}C (‰) in unamended surface layer, 15 days after pulse 1. The
895 intercept for the deep layers (transition and permafrost) model represents soil respired Δ^{14}C (‰) in unamended transition layer, 15 days after
896 pulse 1. Coefficients represent effect size on intercept, and significant effects are bolded.
897

Response variable	Full model	Final Model	Variable	Coefficient	Min CI	Max CI
Soil respired Δ^{14}C (‰)	Treatment x DOI	Intercept	Intercept (Unamended, Surface, DOI 15)	42.4	34.8	50.1
Soil respired Δ^{14}C (‰)	Treatment x Layer x DOI	Treatment	Intercept (Unamended, Transition, DOI 15)	-200.9	-295.9	-109.7
		Layer	**Glucose**	**115.4**	**25.1**	**206.3**
		DOI	Cellulose	30.4	-55.5	118.2
		Layer x DOI	DOI 105	-59.5	-121.0	1.4
			DOI 319	-20.1	-76.8	36.8
			Permafrost x DOI 15	**-224.8**	**-314.8**	**-133.3**
			Permafrost x DOI 105	**158.5**	**65.3**	**253.9**
			Permafrost x DOI 319	44.4	-51.7	138.5

898

42

899 Table 3. Cumulative substrate C loss as a percent (% ± SE) of added substrate (3.5 mg substrate C per g initial C) 105 days after each amendment
900 pulse.

	Pulse 1		Pulse 2		Pulse 3	
	Glucose	**Cellulose**	**Glucose**	**Cellulose**	**Glucose**	**Cellulose**
Surface	54.4 ± 3.9	NA	39.9 ± 2.4	20.0 ± 2.4	45.9 ± 6.8	25.9 ± 2.0
Transition	58.3 ± 15.0	NA	37.8 ± 7.6	15.6 ± 6.8	36.9 ± 11.7	24.5 ± 5.5
Permafrost	125.9 ± 49.0	NA	67.5 ± 32.2	9.4 ± 2.3	80.2 ± 39.8	11.8 ± 5.8

901
902

903 Table 4. Seven-day cumulative substrate C loss as a percent (% ± SE) of respired substrate 105 days after each amendment pulse

| | *Pulse 1* | | *Pulse 2* | | *Pulse 3* | |
	Glucose	Cellulose	Glucose	Cellulose	Glucose	Cellulose
Surface	37.9 ± 2.1	NA	40.7 ± 1.8	5.6 ± 0.7	43.4 ± 4.2	6.9 ± 0.5
Transition	13.8 ± 2.4	NA	29.0 ± 5.6	5.6 ± 1.1	24.2 ± 1.9	4.8 ± 0.5
Permafrost	46.6 ± 3.9	NA	47.4 ± 3.7	6.0 ± 1.7	20.0 ± 1.7	5.2 ± 0.9

904
905

44

906   Supplementary Materials

907

908   Table 1. Glucose and cellulose $\delta^{13}C$ values (‰) by pulse and round. These $\delta^{13}C_{substrate}$ values were used as end-members in the isotopic mass
909   balance equation to calculate priming (Equation 1).

	Pulse 1		Pulse 2		Pulse 3	
	Round 1	Round 2	Round 1	Round 2	Round 1	Round 2
Glucose	73.4	68.9	115.2	98.6	92.0	113.5
Cellulose	8.8	-21.2	76.4	234.1	494.9	494.9
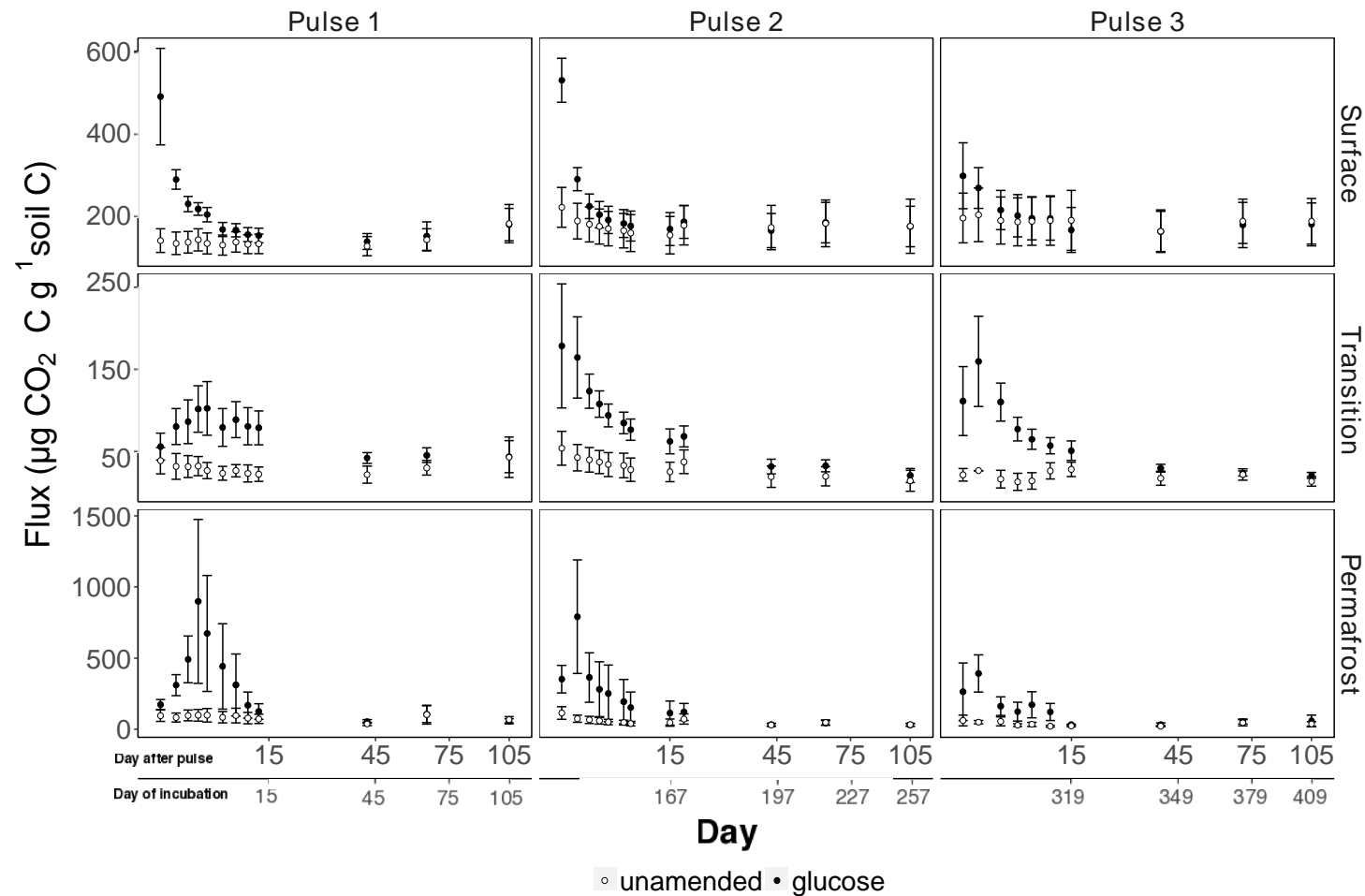
910
911 Figure 1. Total respired C (μg CO_2-C g^{-1}C) in unamended and glucose treatments in surface, transition, and permafrost layers over time (in days)
912 after glucose pulse amendment (DAP) (primary x-axis). The secondary x-axis indicates day since the start of incubation (DOI). The x-axis was
913 square-root transformed to make it easier to see values in the first 15 DAP. Bars are one standard error from the mean. Note that the scale for
914 the y-axis is different for each layer.

46
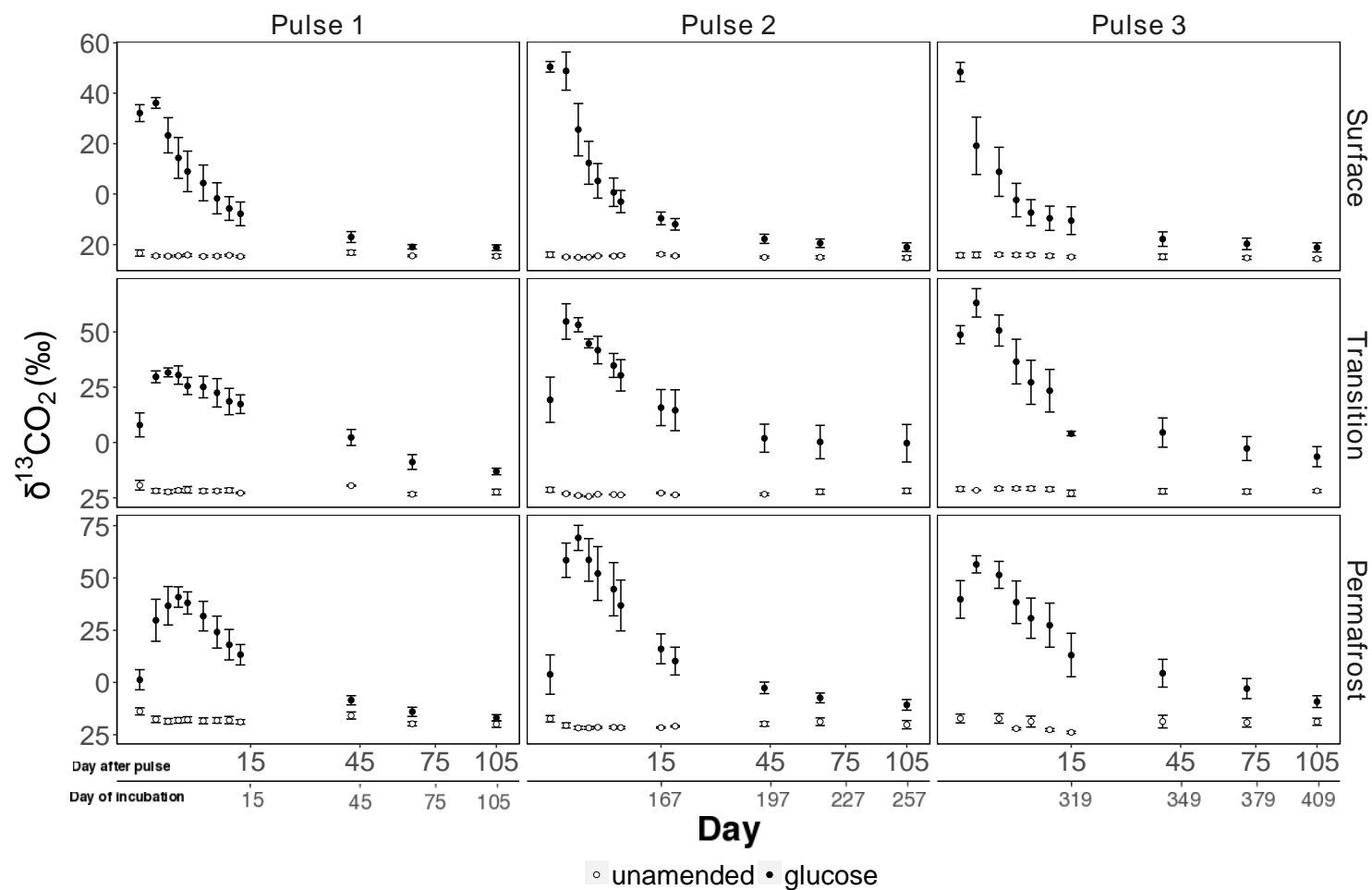
Figure 2. Total respired $\delta^{13}CO_2$-C (‰) in unamended and glucose treatments in surface, transition, and permafrost layers over time (in days) after each glucose pulse amendment (DAP) (primary x-axis). The secondary x-axis indicates day since the start of incubation (DOI). The x-axis was square-root transformed to make it easier to see values in the first 15 DAP. Bars are one standard error from the mean. Note that the scale for the y-axis is different for each layer.
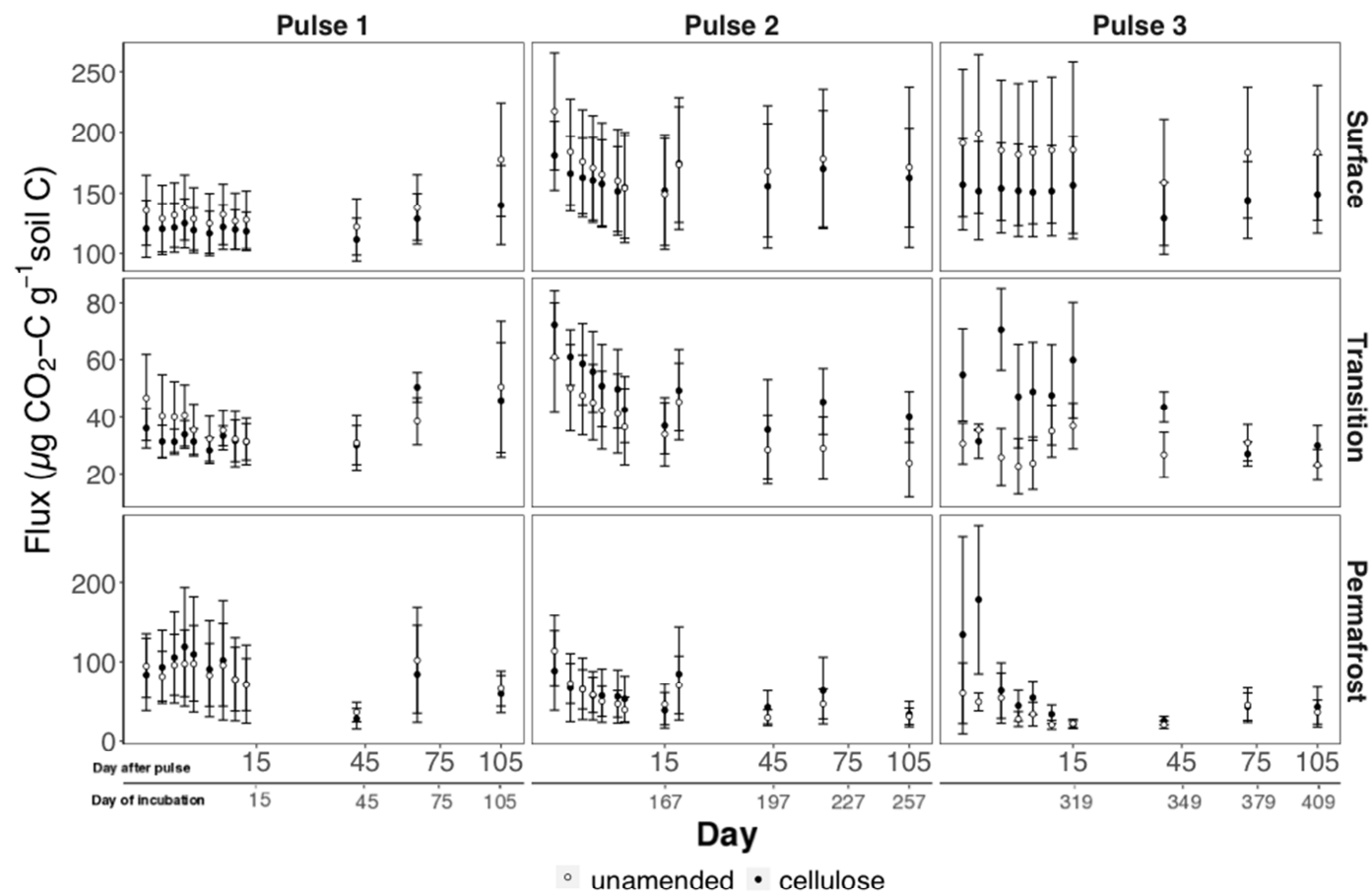
Figure 3. Total respired C (µg CO_2-C g^{-1}C) in unamended and cellulose treatments in surface, transition, and permafrost layers over time (in days) after each cellulose pulse amendment (DAP) (primary x-axis). The secondary x-axis indicates day since the start of incubation (DOI). The x-axis was square-root transformed to make it easier to see values in the first 15 DAP. Bars are one standard error from the mean. Note that the scale for the y-axis is different for each layer.

48

925

926
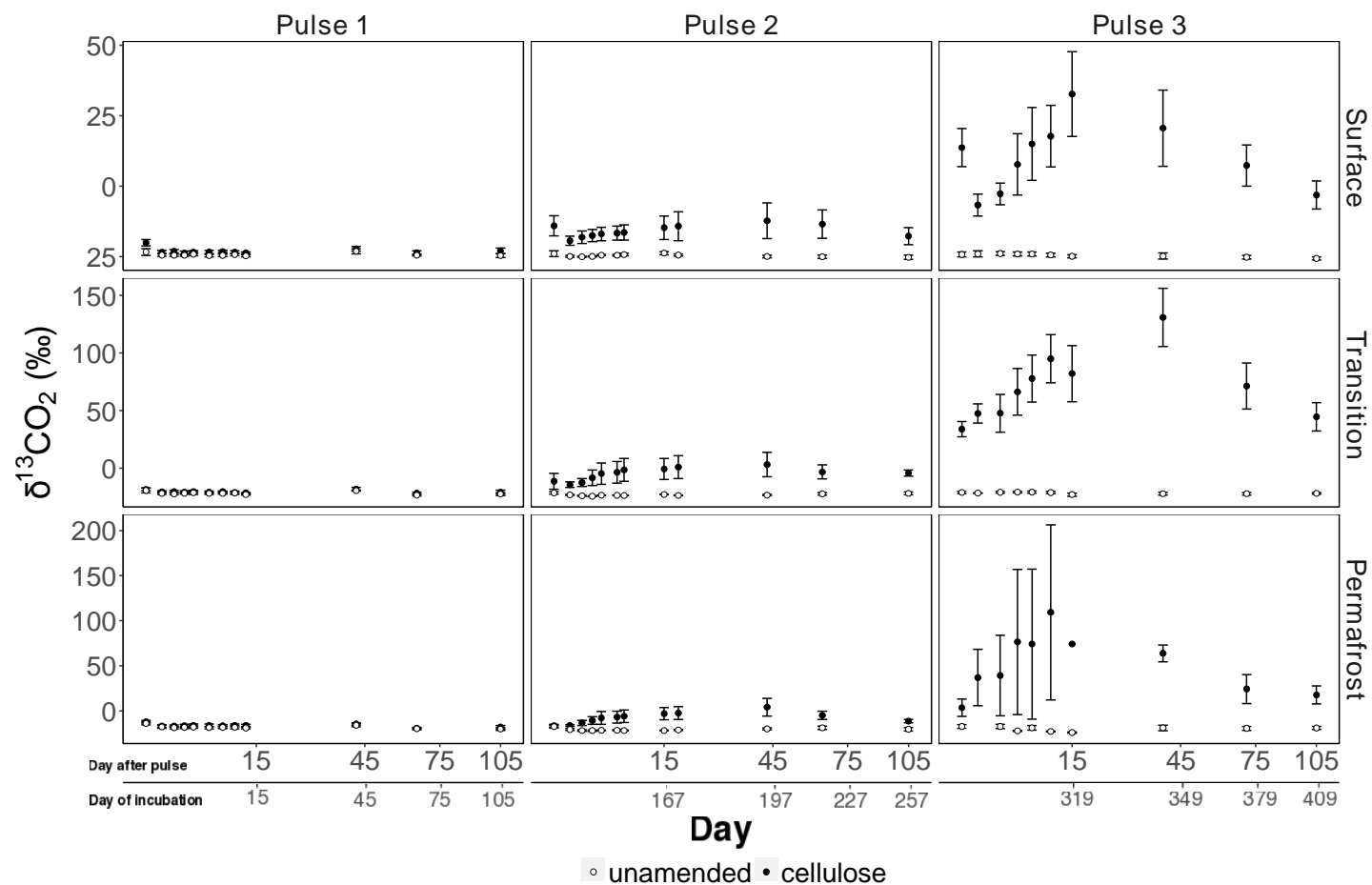
927 Figure 4. Total respired $\delta^{13}CO_2$-C (‰) in unamended and cellulose treatments in surface, transition, and permafrost layers over time (in days)
928 after each cellulose pulse amendment (DAP) (primary x-axis). The secondary x-axis indicates day since the start of incubation (DOI). The x-axis
929 was square-root transformed to make it easier to see values in the first 15 DAP. Bars are one standard error from the mean. Note that the scale
930 for the y-axis is different for each layer.

931 Table 2. Mixed linear effects model parameters for glucose and cellulose priming effects following each amendment pulse. Coefficients
932 represent daily priming values in micrograms CO_2-C per gram soil C, calculated from the effect size on the intercept. The intercept for the
933 glucose model is: unamended surface soil, at 1 DAP, Pulse 1. The intercept for the cellulose is: unamended surface soil, at 1 DAP, Pulse 2. If the
934 Min and Max CI do not overlap zero, it indicated a significant priming response (bolded).

Response variable	Full model	Final Model	Variable	Coefficient	Min CI	Max CI
Glucose priming	Pulse x DAP x Layer	Pulse	Intercept (Surface, 1 DAP, Pulse 1)	5.72	-22.81	35.11
(μg CO_2-C g^{-1}C)		DAP	**Surface x 2 DAP**	**-42.55**	**-77.36**	**-9.09**
		Layer	Surface x 3 DAP	-17.06	-52.17	17.95
		Layer x DAP	Surface x 4 DAP	14.65	-19.95	49.98
		DAP x Pulse	Surface x 5 DAP	13.08	-21.63	46.59
			Surface x 7 DAP	1.43	-35.14	37.75
			Surface x 9 DAP	-2.47	-36.48	31.33
			Surface x 11 DAP	-1.58	-37.7	34.03
			Surface x 13 DAP	-1.38	-37.29	33.13
			Surface x 43 DAP	7.04	-27.38	40.73
			Surface x 65 DAP	5.73	-29.03	41.46
			Surface x 105 DAP	-5.28	-40.28	29.68
			Transition x 1 DAP	21.97	-19.71	63.46
			Transition x 2 DAP	-9.57	-55.91	37.76
			Transition x 3 DAP	16.71	-30.07	63.26
			Transition x 4 DAP	36.23	-8.14	81.07
			Transition x 5 DAP	29.37	-14.72	73.26
			Transition x 7 DAP	19.01	-25.73	64.79
			Transition x 9 DAP	11.7	-32.26	55.02
			Transition x 11 DAP	9.54	-34.46	52.97
			Transition x 13 DAP	10	-33.56	56.6
			Transition x 43 DAP	14.03	-30.81	59.23

50

Transition x 65 DAP	10.11	-34.3	54.93
Transition x 105 DAP	-1.91	-44.87	43.74
Permafrost x 1 DAP	**91.32**	**58.46**	**123.17**
Permafrost x 2 DAP	**86.82**	**47.35**	**126.75**
Permafrost x 3 DAP	**60.71**	**24.09**	**97.09**
Permafrost x 4 DAP	**67.59**	**31.23**	**102.93**
Permafrost x 5 DAP	**58.44**	**22.32**	**95.47**
Permafrost x 7 DAP	**64.78**	**29.39**	**101.69**
Permafrost x 9 DAP	24.3	-12.62	61.34
Permafrost x 11 DAP	35.9	-0.6	73.03
Permafrost x 13 DAP	15.3	-21.07	54.35
Permafrost x 43 DAP	11.36	-25.44	48.13
Permafrost x 65 DAP	6.53	-29.06	42
Permafrost x 105 DAP	-1.99	-38.56	34.79
1 DAP x Pulse 2	**55.88**	**26.56**	**84.08**
1 DAP x Pulse 3	**-41.04**	**-69.06**	**-12.55**
2 DAP x Pulse 2	-18.44	-58.19	21.76
2 DAP x Pulse 3	-22.35	-75.37	28.72
3 DAP x Pulse 2	-28.33	-68.56	12.56
3 DAP x Pulse 3	-40.58	-83.53	0.74
4 DAP x Pulse 2	-18.96	-59.58	22.15
4 DAP x Pulse 3	-19.86	-61.09	20.33
5 DAP x Pulse 2	-12.65	-51.59	28.02
5 DAP x Pulse 3	1.96	-38.03	42.87
7 DAP x Pulse 2	-14.95	-53.87	24.24
7 DAP x Pulse 3	6.44	-36.06	46.97
9 DAP x Pulse 2	0.08	-39.62	40.83

51

			9 DAP x Pulse 3	1.36	-39.49	41.22
			11 DAP x Pulse 2	5.8	-34.07	47.4
			11 DAP x Pulse 3	5.47	-35.19	45.21
			13 DAP x Pulse 2	8.39	-30.88	48.36
			13 DAP x Pulse 3	4.57	-35.24	43.76
			43 DAP x Pulse 2	-1.06	-39.76	40.23
			43 DAP x Pulse 3	4.07	-36.41	45.1
			65 DAP x Pulse 2	1.81	-38.27	41.99
			65 DAP x Pulse 3	0.79	-40.75	40.81
			105 DAP x Pulse 2	2.72	-38.06	42.82
			105 DAP x Pulse 3	8.25	-33.1	49.37
Cellulose priming	Pulse x DAP x Layer	Pulse	Intercept (Surface, Pulse 2)	-16.87	-46.95	12.78
(μg CO_2-C g^{-1}C)		Layer	**Surface x Pulse 3**	**-42.54**	**-49.41**	**-34.94**
		Pulse x Layer	Transition x Pulse 2	4.97	-43.03	51.4
			Transition x Pulse 3	8.85	-0.02	24.77
			Permafrost x Pulse 2	-1.7	-38.22	35.93
			Permafrost x Pulse 3	**8.29**	**7.66**	**28.67**

935
936

52

937   Table 3. Average respired delta [13]C (± SE) in unamended soils for the entire duration of the incubation experiment. Values not sharing the same
938   letter indicate a significant difference.

	$\delta^{13}CO_2$ (‰)
Surface	-24.47 ± 0.07[a]
Transition	-21.99 ± 0.17[b]
Permafrost	-18.95 ± 0.20[c]

939

940

Title: Glucose addition increases the magnitude and decreases the age of soil respired carbon in a long-term permafrost incubation study

Authors: Elaine Pegoraro[a,b], Marguerite Mauritz[a,b], Rosvel Bracho[c], Chris Ebert[a,b], Paul Dijkstra[a,b], Bruce A. Hungate[a,b], Kostas T. Konstantinidis[d], Yiqi Luo[a,b,e,g], Christina Schädel[a.b], James M. Tiedje[f], Jizhong Zhou[g], Edward A.G. Schuur[a,b].

Highlights:

Glucose addition increased permafrost soil C loss two-fold.

Glucose addition to surface soils did not elicit a priming response.

Cellulose addition to surface soils elicited a negative priming response.

Glucose addition decreased the age of soil-respired carbon in deep layers.